WTMA-3000A WIND TURBINE DESIGN PROJECT REPORT

25-Dec-15

Wind Energy and wind Turbine Technology

Designers and Authors: Waheedullah Taj and Mehmet Aksay

ABSTRACT

A 3 bladed 3 MW Horizontal Axis Wind Turbine (HAWT) is designed. Aerodynamic design is based on Blade Element Momentum (BEM) Theory. Structural elements are designed using simple beams at first and super fine mesh Finite Element Model later in the design procedure.

The turbine is designed for an IECIII wind velocity standard.

Wind turbine graphs and diagrams such as the graph of coefficient of power versus tip speed ratio, coefficient of thrust versus tip speed ratio and power versus wind speed curves are drawn at the end of the report.[1]

TABLE OF CONTENTS

NOMENCLATURE

WT	Wind Turbine
HAWT	Horizontal Axis Wind Turbine
VAWT	Vertical Axis Wind Turbine
IEC	International Electrochemical Commission
BEM	Blade Element Momentum Theory
a	Axial Induction Factor
a’	Radial Induction Factor
TSR	Tip Speed Ratio
C_p, C_p	Coefficient of Power
C_T, C_T	Coefficient of Thrust

PART 1
AERODYNAMIC DESIGN

1.1 INTRODUCTION

It is no secret that global warming and climate change are choking every hope that we had in a continuous, endless and comfortable life on earth. Environmental cataclysms such as tornadoes, typhoons, tsunamis and floods are increasing at alarming rates. The core reason for climate change is the colossal amounts of greenhouse gases such as carbon dioxide that are being released to the atmosphere. Most of this emission comes from traditional power production facilities such as fossil fuel power plants. To overcome this burden humanity is looking for renewable sources of energy. Renewable sources of energy are generally very clean and harmless with next to zero greenhouse gas emissions and disasters.

One of the shining stars of the renewable energy world is wind energy. Wind energy has definitely established itself as an integral part of power production in today's world. A significant interest is being drawn to wind turbines by government agencies and as a result installed wind power capacity has risen from mere 6.1 GW in 1996 to 369.6 GW in 2014. Although the rise in usage of wind power is definitely significant, there is still a long way to go.

This report summarizes the procedure that was undertaken while designing a 3 MW Horizontal Axis Wind Turbine (HAWT) with 3 blades. A HAWT, as the name suggests, is a wind turbine whose axis of rotation is horizontal, as opposed to Vertical Axis Wind Turbines (VAWT) whose axis of rotation is vertical.

The wind turbine will be optimized for International Electrotechnical Commission (IEC) III class wind speed. According to IEC a class III wind speed has a maximum annual average wind speed of 7.5 m/s, 50-year return gust of 50 m/s and 1-year return gust of 39.4 m/s [2]. For the purposes of this report annual average wind speed will be taken to be 7.5 m/s.

1.2 COMPETITOR STUDY

As any other design procedure, the design of a wind turbine starts with a competitor study. In competitor study a set of products of the same category and class as the one being designed are researched and key design parameters relating to them are gathered. Such a study can be very helpful in finding meaningful values for initial guesses of such parameters. Some 3 MW wind turbines readily available in the market were gathered and their key (publicly available) properties are tabulated below

Name	Wind Speed Class	Rotor Diameter (m)	Rated Power (kW)	Cut-in Speed (m/s)	Cut-out Speed (m/s)	Max Chord (m)	Tip Speed Ratio	Hub Height (m)
Vestas V105	IEC I	105	3450	3	25	4	NA	72.5
Vestas V90	IEC II	90	3000	3.5	25	3.5	5.88	105
Nordex N100	IEC I	99.8	3300	3.5	25	NA	7.47	100
Vestas V112	IEC I	112	3450	3	25	4	8.6	94
Nordex N131	IEC III	131	3000	3	20	NA	5.88	114

Table 1: Competitor wind turbine data.

1.2.1 Rotor Diameter

1.2.1.1 Competitor Data

Average rotor diameter of the competitors read (after linear extrapolation for power correction and mean wind speed correction):

$$D_{ave} = \frac{105\left(\frac{3000}{3450}\right)^{1/2}\left(\frac{10.0}{7.5}\right)^{3/2} + 90\left(\frac{3000}{3000}\right)^{1/2}\left(\frac{8.5}{7.5}\right)^{3/2} + 99.8\left(\frac{3000}{3300}\right)^{1/2}\left(\frac{10.0}{7.5}\right)^{3/2}}{3} + \frac{+112\left(\frac{3000}{3450}\right)^{1/2}\left(\frac{10.0}{7.5}\right)^{3/2} + 131\left(\frac{3000}{3000}\right)^{1/2}\left(\frac{7.5}{7.5}\right)^{3/2}}{2} = 132$$

$$R = \frac{D}{2} = 66\ m \qquad (1)$$

Note that correction factors for power have powers of ½ and those of mean wind speed 3/2. This is because when everything else is fixed rotor diameter changes with square root of power and three square roots of velocity respectively. Also note that velocities of 10.0 m/s and 8.5 m/s correspond to mean wind speeds of IEC I and IEC II classes respectively. This is clarified with the equations below:

$$P \approx AV^3 \approx D^2V^3$$
$$D \approx \sqrt{P}\sqrt{V^{-3}}$$
$$D_2 = D_1\sqrt{\frac{P_2}{P_1}}\sqrt{\frac{V_1^3}{V_2^3}} \qquad (2)$$

Where subscripts 1 and 2 denote two hypothetical wind turbines.

1.2.1.2 Classical Equations

Modern wind turbines have a power coefficient of around 0.45. Using this and the power equation given below

$$P = \frac{1}{2}\rho V^3 S C_p = \frac{\pi}{2}\rho V^3 R^2 C_p \qquad (3)$$

Where P = 3000 MW, ρ=1.225 kg/m^3, V = 7.5 m/s, C_p = 0.45. Then radius is calculated to be R = 90 m. While it is true that the performance of the commercial turbines might be hyped, we also need to consider the fact that with a radius of 90 m the wind turbine will produce 3 MW at exactly 7.5 m/s wind speed. At higher speeds the power production will not increase because the rated power of the turbine is 3 MW. This means most of wind power is not harvested, instead it only helps decrease the structural life of the turbine. However if we choose a blade radius of 66 m although the wind turbine will not produce 3 MW of power at a wind speed of 7.5 m/s, it will generate much more power per unit cost or weight. As a consequence of this reasoning a blade radius of **66 m** was chosen for this wind turbine.

1.2.2 Tip Speed Ratio

Average tip speed ratio of the competitors yields λ = 6.96. Historical trends however, indicate a value of λ = 4 for such a wind turbine. Mathematically the higher the tip speed ratio the better. However historically high values of tip speed ratio were avoided due to structural problems. The authors of this report however are inclined that the technological advancements in the last decade in the field of wind turbine rotor structures and materials allow for higher values of tip speed ratio too. Thus a value of **λ = 6** will be selected as a weighted compromise between historical trends and competitor data.

1.3 AIRFOIL SELECTION

Airfoil selection is one of the most important issues in Wind Turbines. Because the aerodynamic forces which create the torque depend on the shape of the airfoil. Lift, drag and lift to drag ratio, leading edge roughness sensitivity, stall characteristics and aeroacoustics are effected by the airfoil shape. The structural issues and manufacturability should be also considered while designing airfoils. Keep in mind that the Re# for this design is between 1000000-3000000 range.

In 80s and early 90s some NACA airfoils were used for wind turbines. However, by experiments it is understood that the thick NACA airfoils used for wind performance had lower performance than expected due to premature transition. This effects were more dominantly seen when the relative thicknesses of the airfoils exceeded %21. In addition to these the leading edge roughness tolerance is an important issue for airfoils of the wind turbines. Because wind turbines always expose to dirt or insects and the performance change should not be much in such a case.

While choosing inboard airfoils due to structural reasons airfoils which has high relative thicknesses (%30-40) were used. In addition, Inboard airfoils requires higher maximum lift coefficient to sustain required torque even for the lower incoming wind speeds.

While choosing outboard airfoils, maximum lift to drag ratio is less important. In addition the design C_l and $C_{l,max}$ should be close to each other to some amount to prevent excessive loads. It should be kept in mind that if C_l and $C_{l,max}$ are too close to each other this may cause stall. From [3] approximately 0.2 difference is sufficient for this difference. A large $C_{l,max}$ is good for outboard airfoils because it decreases the required chord length, but in case of small large $C_{l,max}$ causes bad stall characteristics. In addition, the

larger the $C_{l,max}$ the more prone the airfoil to leading edge surface roughness. Due to these reasons the $C_{l,max}$ value for outboard airfoil should be at a certain value range.

In addition to all these, the experimental results for airfoils are investigated due to possible inaccuracies expected from softwares such as XFLR5.

Keeping these considerations in mind three different airfoils are chosen for the 3MW wind Turbine designed:

Airfoil	Clean Airfoil					Airfoil with LE roughness	
	t/c	α_0(deg)	$C_{l,\ \alpha}$	$C_{l,max}$	$(C_l/c_d)_{max}$	$C_{l,max}$	$(C_l/c_d)_{max}$
DU 93-W-300	0.30	-2.20	0.128	1.56	98	1.17	53
DU 91-W2-250	0.25	-3.2	0.126	1.37	128	1.16	62
DU 93-W-210	0.21	-4.2	0.123	1.35	143	1.17	54
DU 95-W-180	0.18	-2	0.116	1.21	143	1.14	70

Table 2: Airfoils from[3]

Here while testing the values for LE roughness a zigzag tape of 0.35 mm thickness is applied at the %5 chord station. The data on the table is got from[3].

The DU 91-W-300 airfoil used as innerboard airfoil while DU 95-W-180 is used for outerboard while DU-250 and DU 95-W-210 is used as intermediate airfoils. Keep in mind that transition from one to another is easier for these airfoils.

1.3.1 DU 97-W-300:

The figures given below are taken from [3]. All are measured at Re=3000000

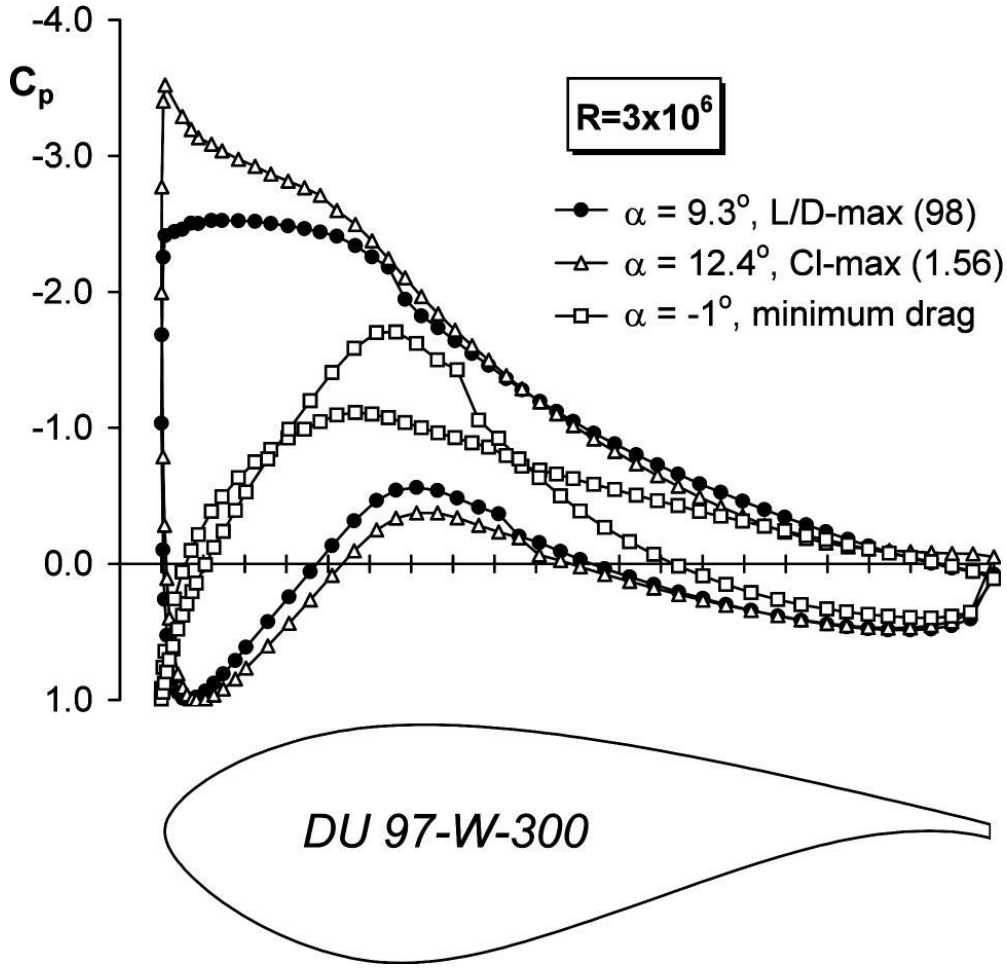

Figure 1: Cp distribution of DU 97-W-300 from [3]

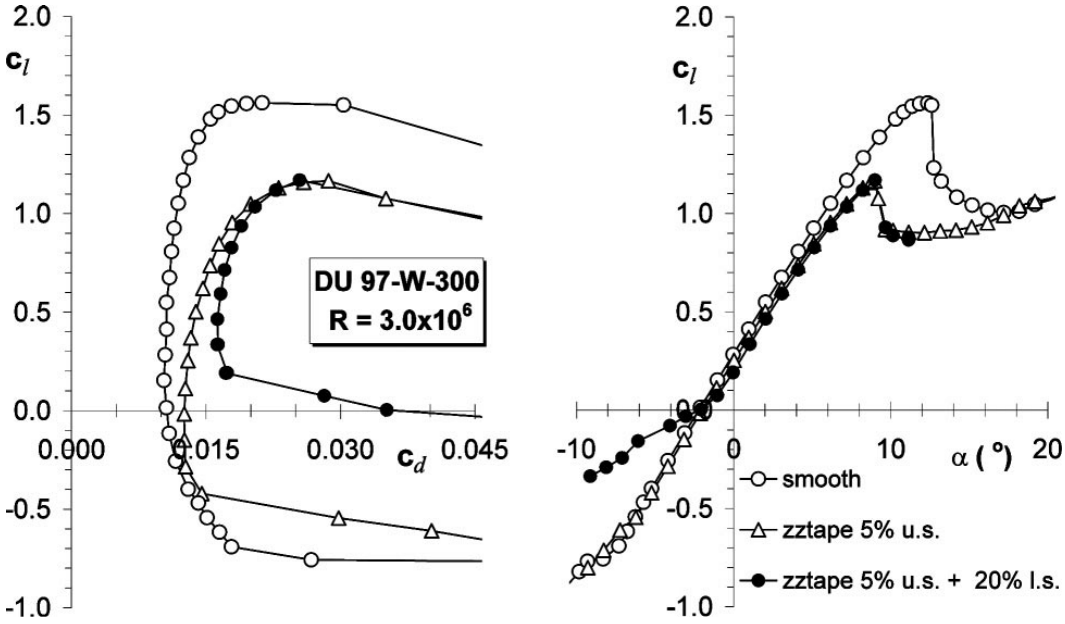

Figure 2:C_l vs C_d and α distribution of DU 97-W-300 from [3]

As seen it has acceptable leading edge surface roughness tolerance for such a thick airfoil and high $C_{l,max}$ value. In addition, this airfoil is good for the transition to DU 93-W-210 airfoil.

1.3.2 DU 91-W2-250:

This airfoil is designed for gradual stall characteristics and high aerodynamic performance. It has maximum thickness around 30%c. The figures below are for this airfoil for Re#=3000000.

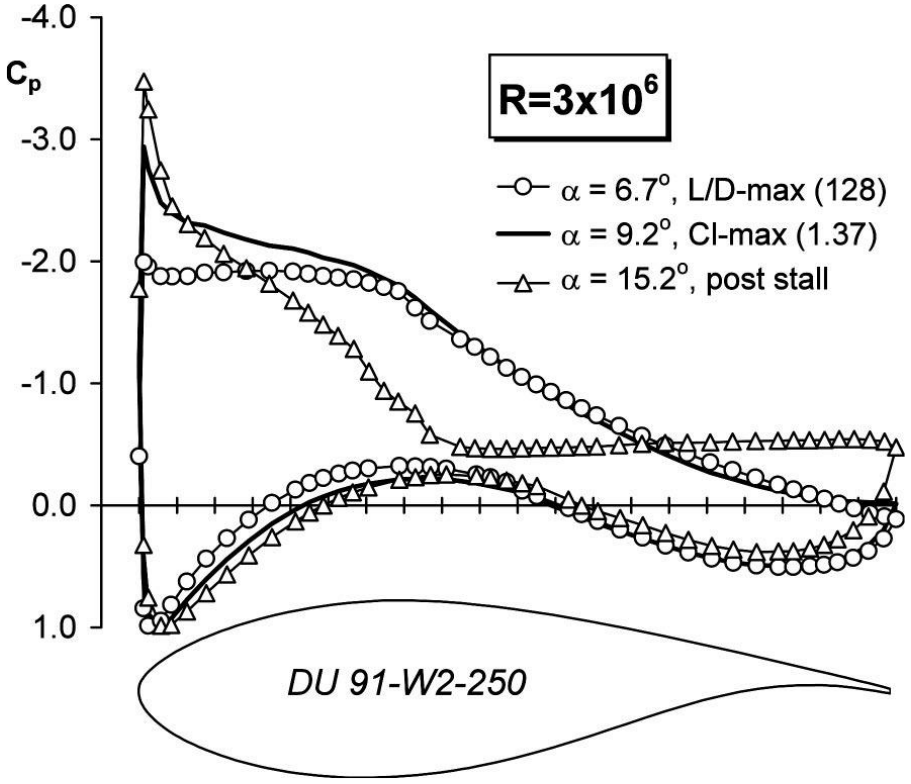

Figure 3: C_P distribution of DU 91-W2-250 from [3]

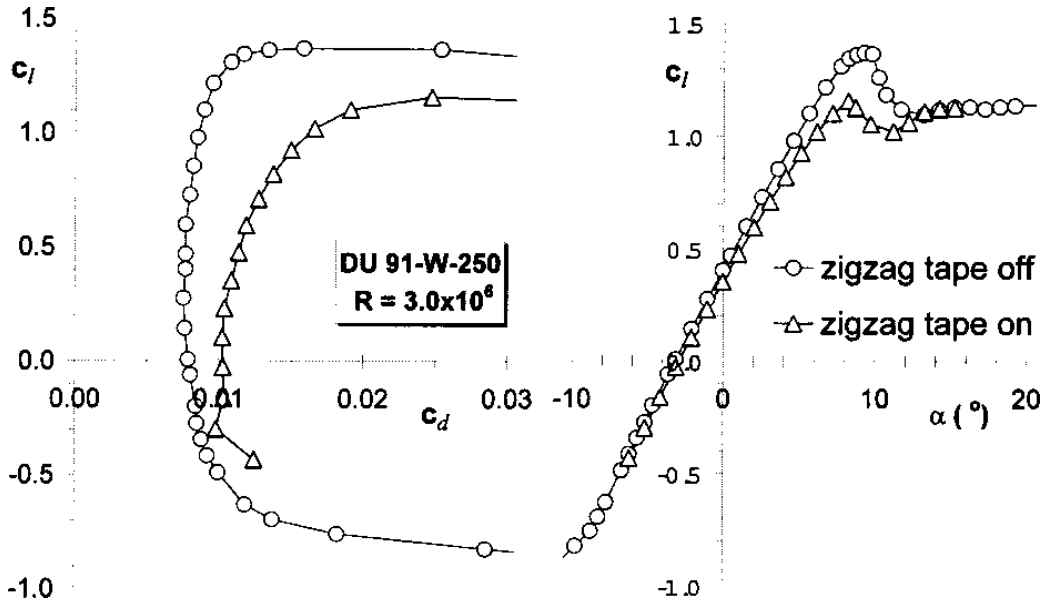

Figure 4: C_l vs C_d and α distribution of DU 91-W2-250 from [3]

1.3.3 DU 93-W-210:

This airfoil is designed as an airfoil to serve between the near root intermediate airfoils such as DU 91-W2-250 and outerboard airfoil. It has a very good leading edge roughness sensitivity compared to similar NACA airfoils. The figure showing necessary values for variety of Re# for this airfoil are given below:

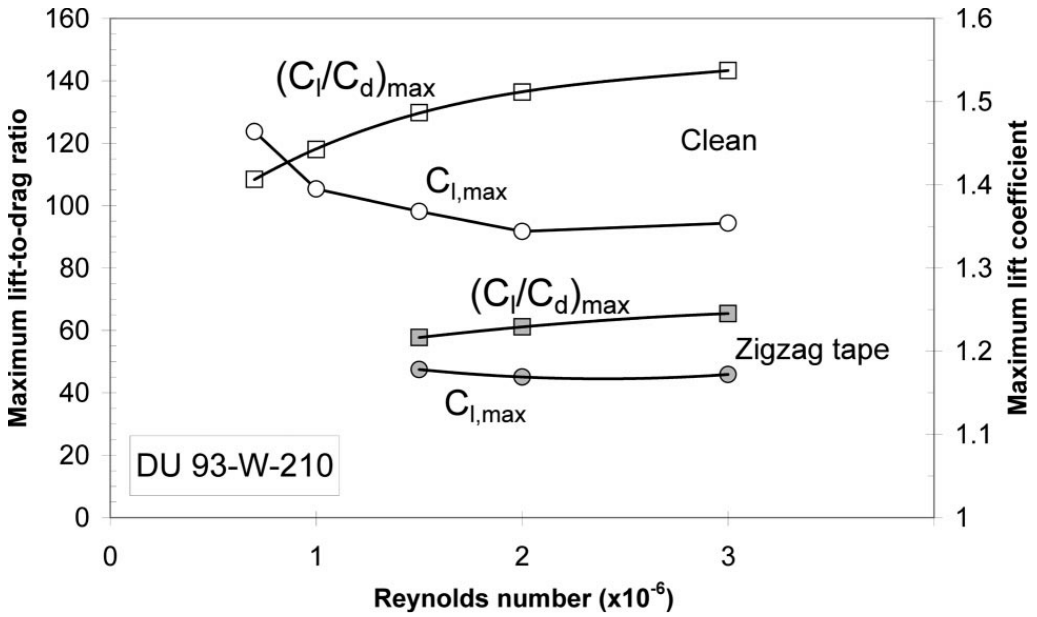

Figure 5: Performance parameters vs Re# of DU 93-W-210 from [3]

1.3.4 DU 96-W-180:

This airfoil has a thin trailing edge to avoid excessive boundary layer noise. It has higher aerodynamic performance than similar airfoils. The figures for Re#=3000000 are given below:

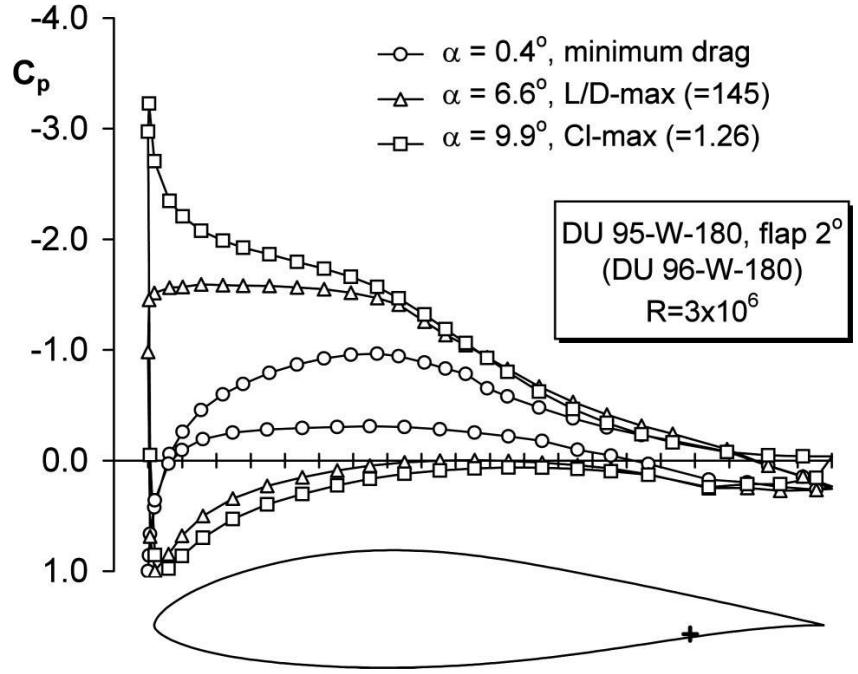

Figure 6: C_p distribution of DU 96-W-180 from [3]

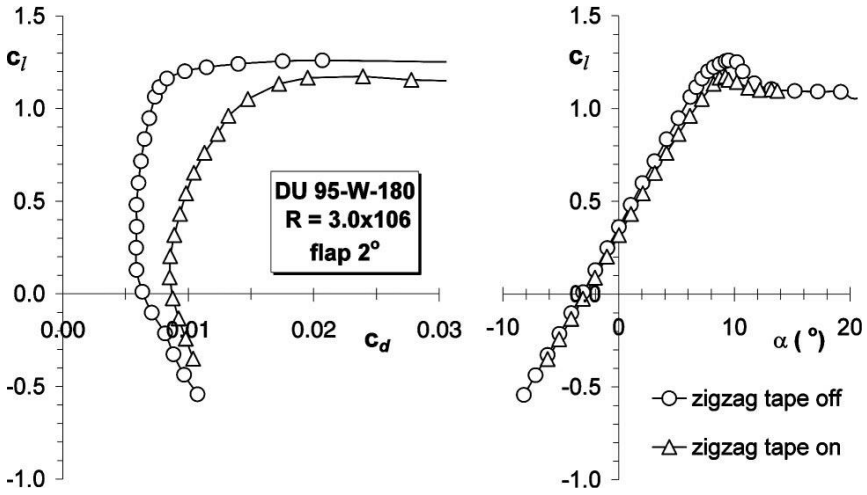

Figure 7: C_l vs C_d and α distribution of DU 96-W-180 from [3]

1.4 CHORD AND TWIST DISTRIBUTION

Chord and twist distributions will be found using classical BEM equations and by employing axial induction factor a and radial induction factor a'. We will initially assume a value for a and a' arbitrarily within their allowed ranges. Then angle of relative wind, φ is given as

$$\varphi = \text{atan}\frac{1-a}{(1+a')\lambda r}\ R \tag{4}$$

Then chord distribution is calculated according to the equation below:

$$c = \frac{8\pi r sin(\varphi) F\left(\cos(\varphi) - \frac{\lambda r}{R}\sin(\varphi)\right)}{BC_l\left(sin\varphi - \frac{\lambda r}{R}cos\varphi\right)} \tag{5}$$

Where F is Prandtl's tip loss function that can be found as shown below:

$$F = \frac{2}{\pi}\text{acos}\left(exp\left(-\frac{\frac{B}{2}\left(1-\frac{r}{R}\right)}{\frac{r}{R}sin\varphi}\right)\right) \tag{6}$$

These optimizations were done using QBlade, an open source wind turbine design software.

The turbine was divided into 16 sections. The first two sections used a circular airfoil for structural reasons. The next four sections use DU 91-W2-250, the four after that use DU 93-W-210 and the sections at the end use DU 95-W-180.

The final shape of the blade is shown in Figure 8.

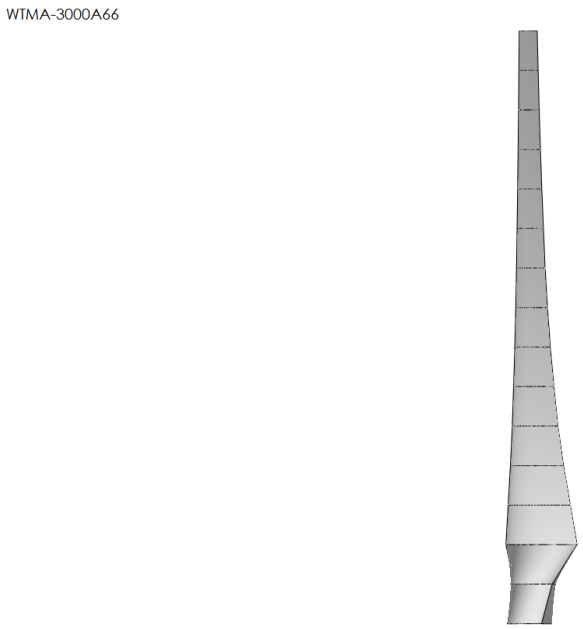

Figure 8: One of the three blades of WTMA-3000A.

Twist, chord and airfoil distributions are given in the table below.

Station	Pos (m)	Chord (m)	Twist (deg)	Airfoil
1	0	5	60.82	Circular
2	4.4	5	36.81	Circular
3	8.8	9.965	12.96	DU97W300LM
4	13.2	8.833	4.86	DU97W300LM

5	17.6	7.67	4.74	DU 91-W2-250
6	22	6.681	6.681	DU 91-W2-250
7	26.4	5.951	0.25	DU 93-W-210
8	30.8	5.291	-1.63	DU 93-W-210
9	35.2	4.752	-3.09	DU 93-W-210
10	39.6	4.306	-4.25	DU 93-W-210
11	44	3.933	-5.2	DU 93-W-210
12	48.4	3.617	-6	DU 93-W-210
13	52.8	3.413	-9.16	DU 95-W-180
14	57.2	3.175	-9.73	DU 95-W-180
15	61.6	2.967	-10.23	DU 95-W-180
16	66	2.784	-10.66	DU 95-W-180

Table 3: Twist and chord distribution of WTMA-3000A.

The following graphs were also generated.

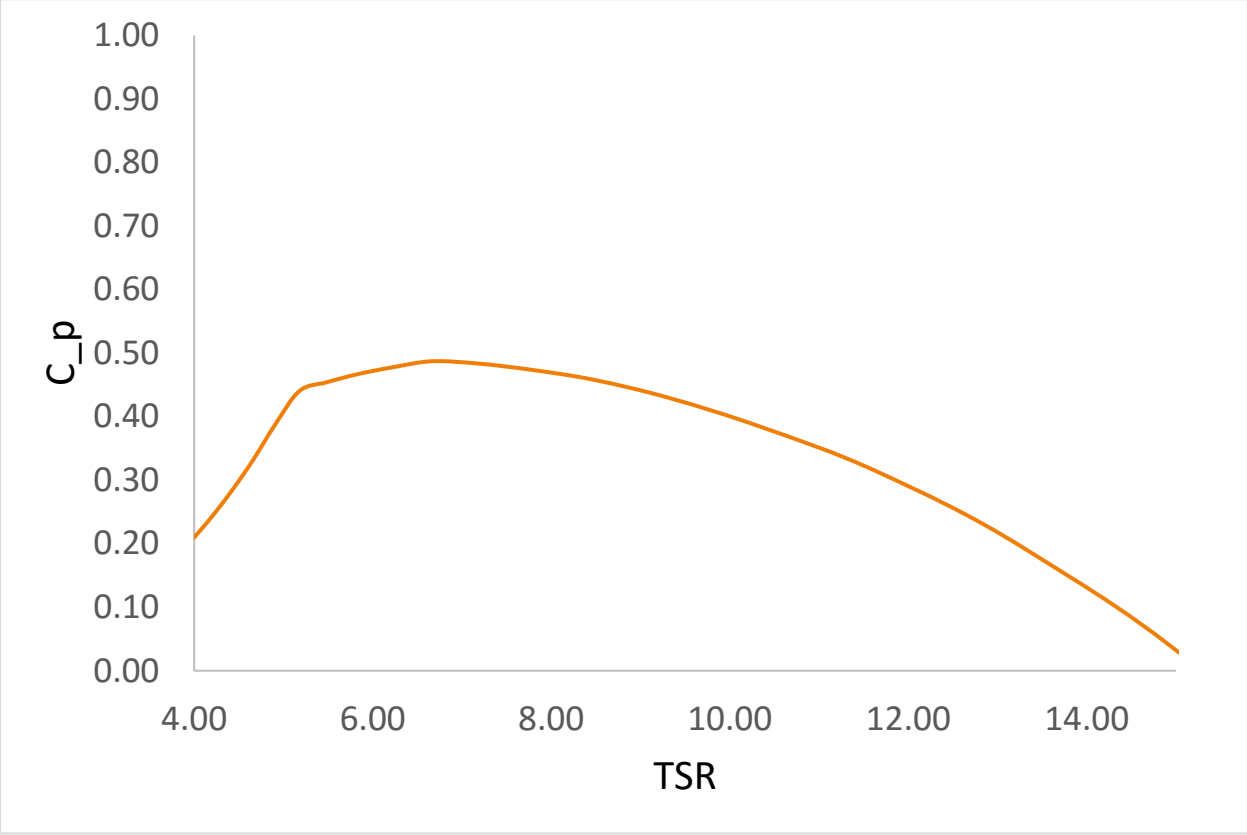

Figure 9: Coefficient of power versus tip speed ratio for WTMA-3000A.

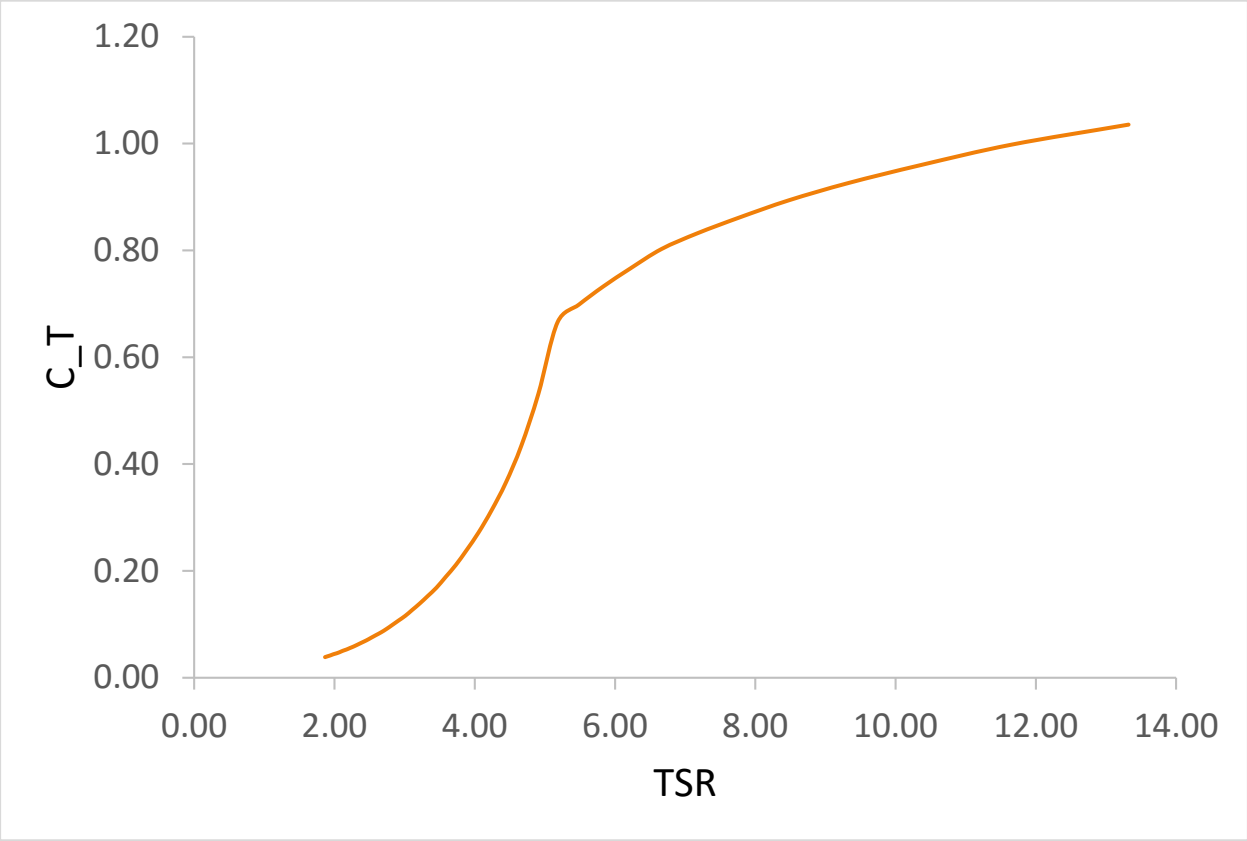

Figure 10: Coefficient of thrust versus tip speed ratio for WTMA-3000A.

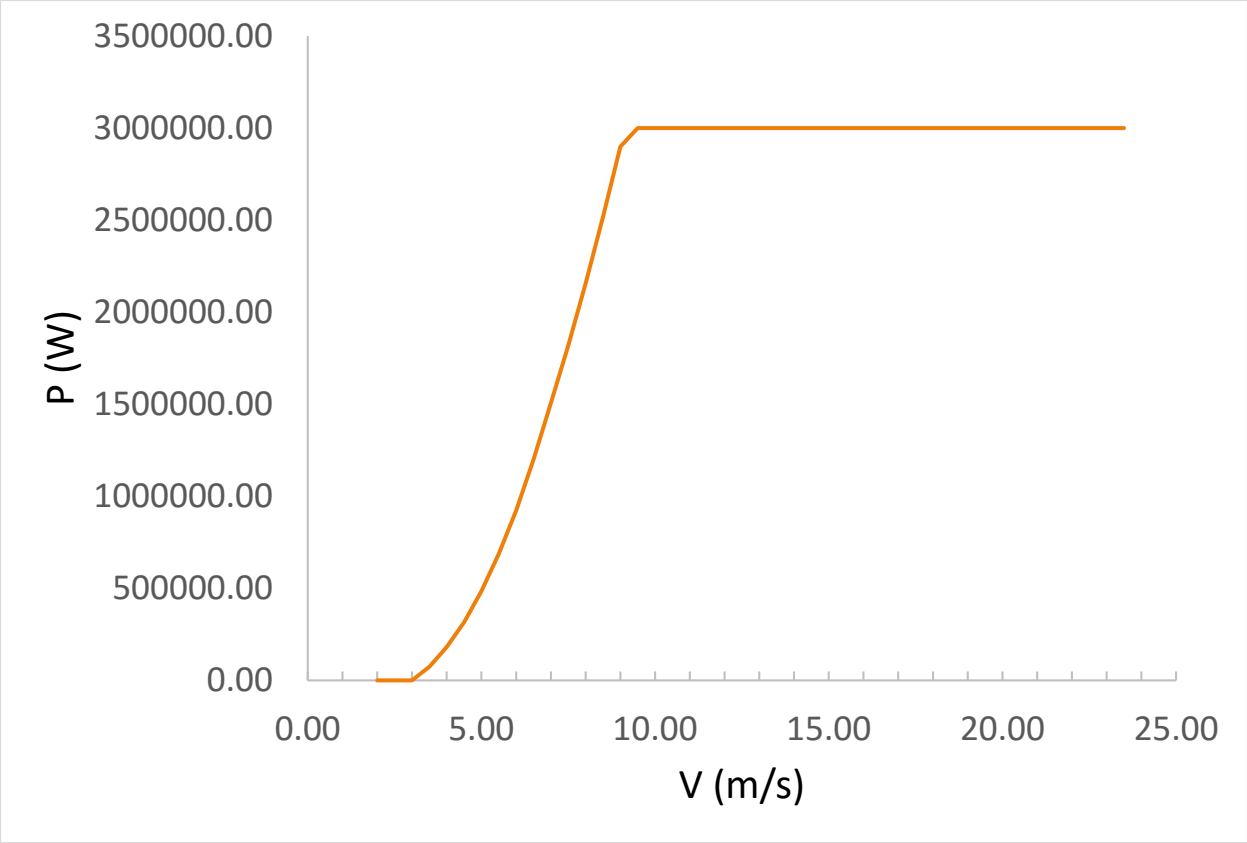

Figure 11: Power generated versus wind speed

The figures below are plotted for Freestream Velocity of 7.5 m/s. And they represent various performance parameters.

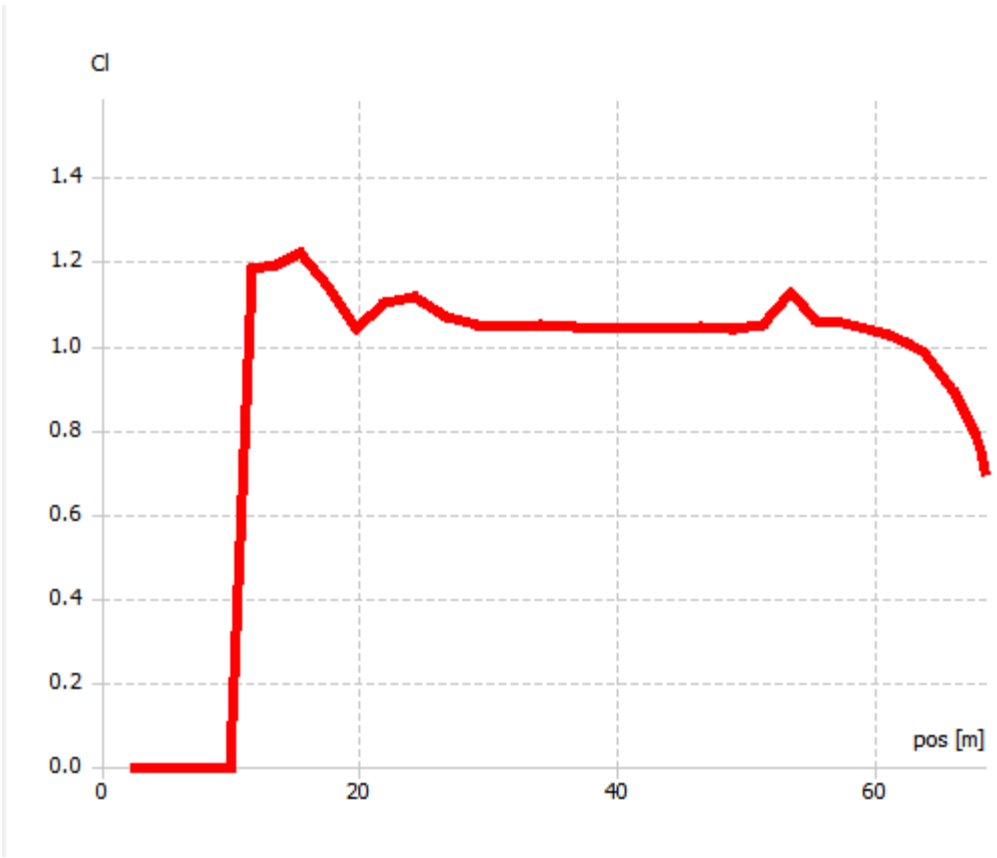

Figure 12:C_l vs span graph

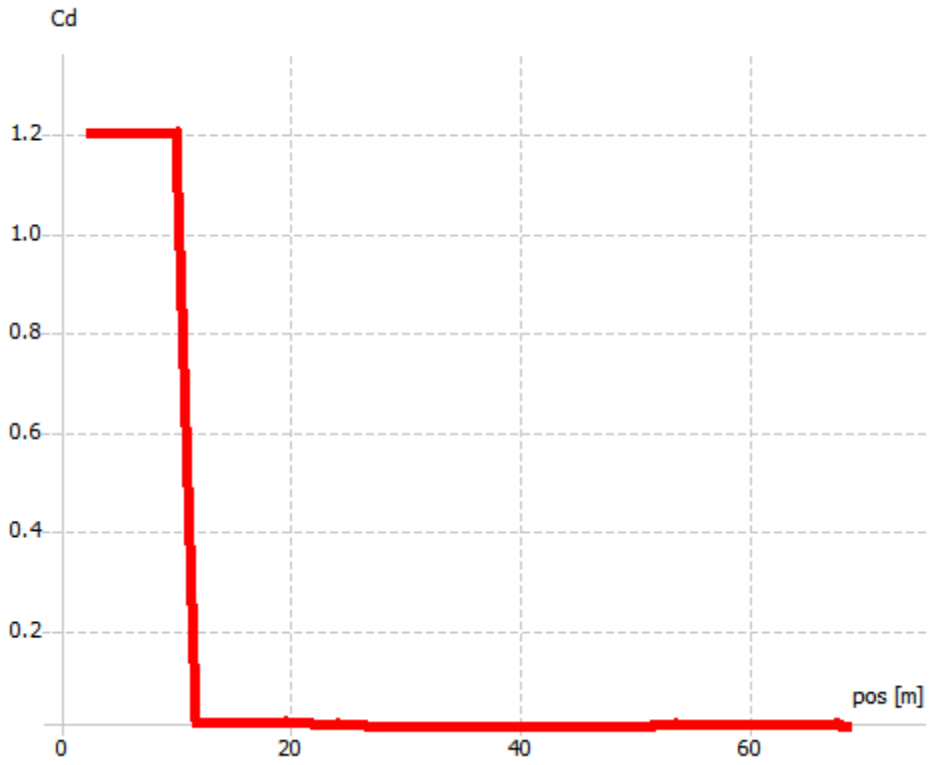

Figure 13:C_d vs span graph

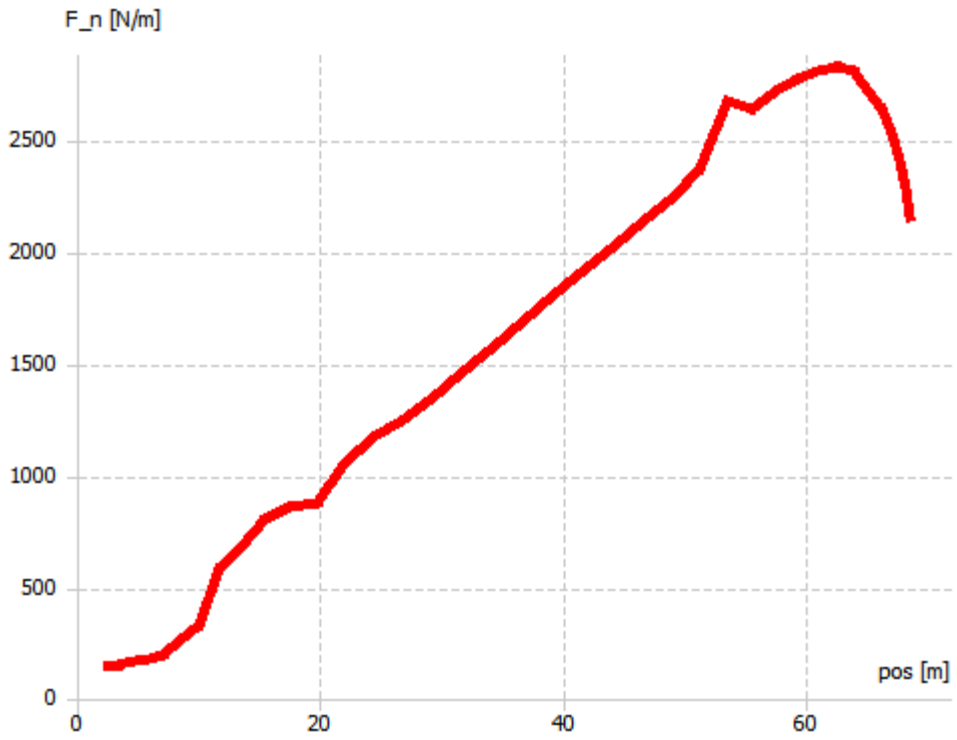

Figure 14:Axial Blade Force vs span graph

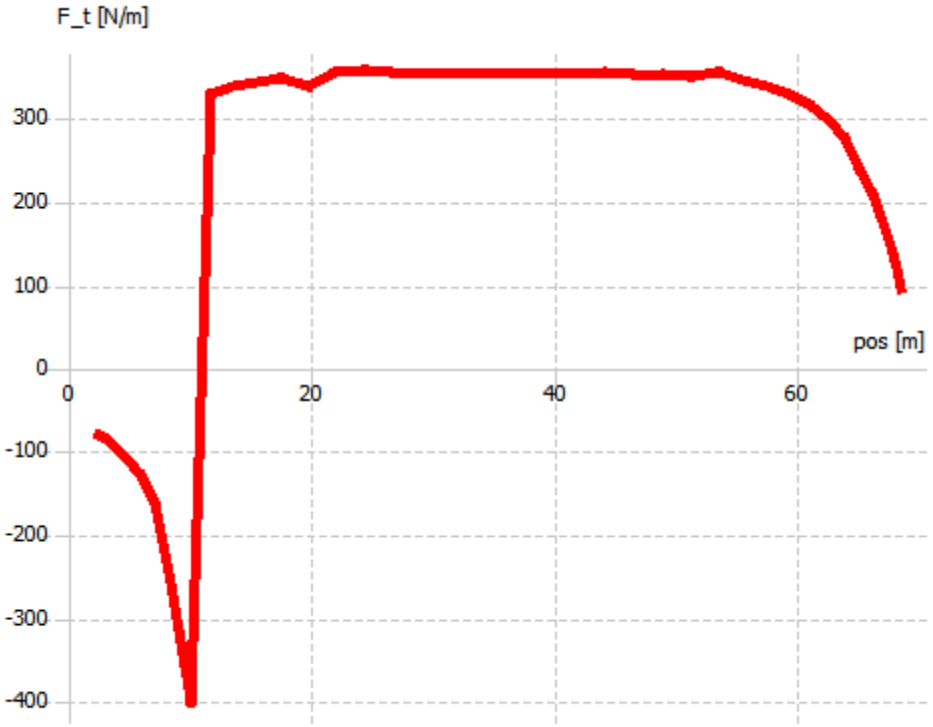

Figure 15:Tangential Blade Force vs span graph

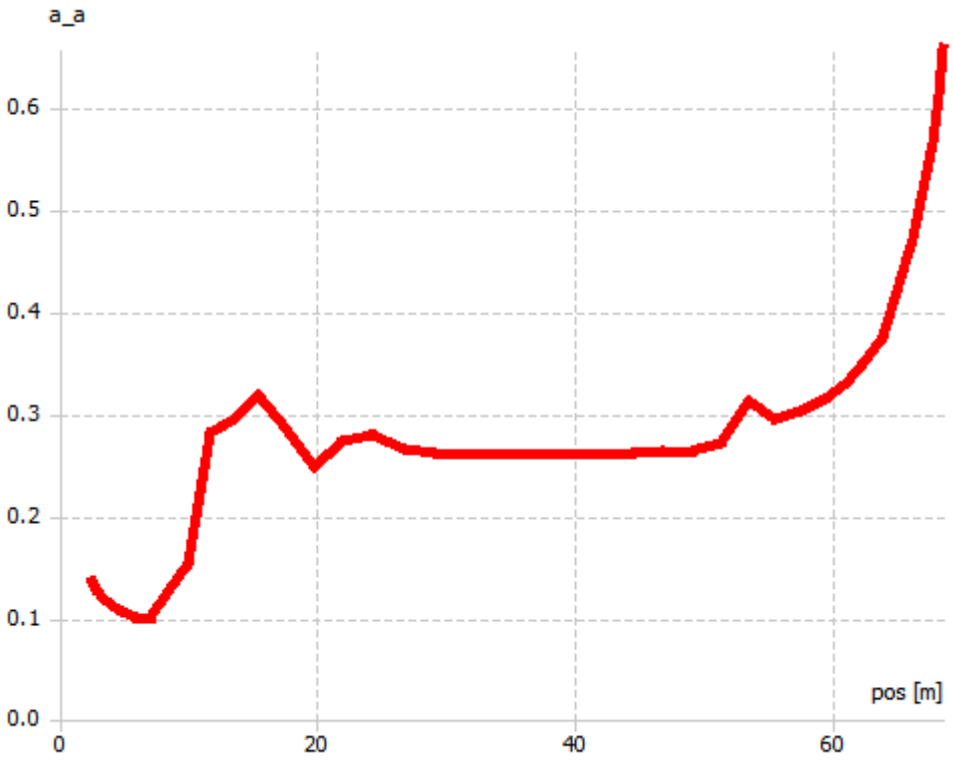

Figure 16:Axial Induction Factor vs Span Graph

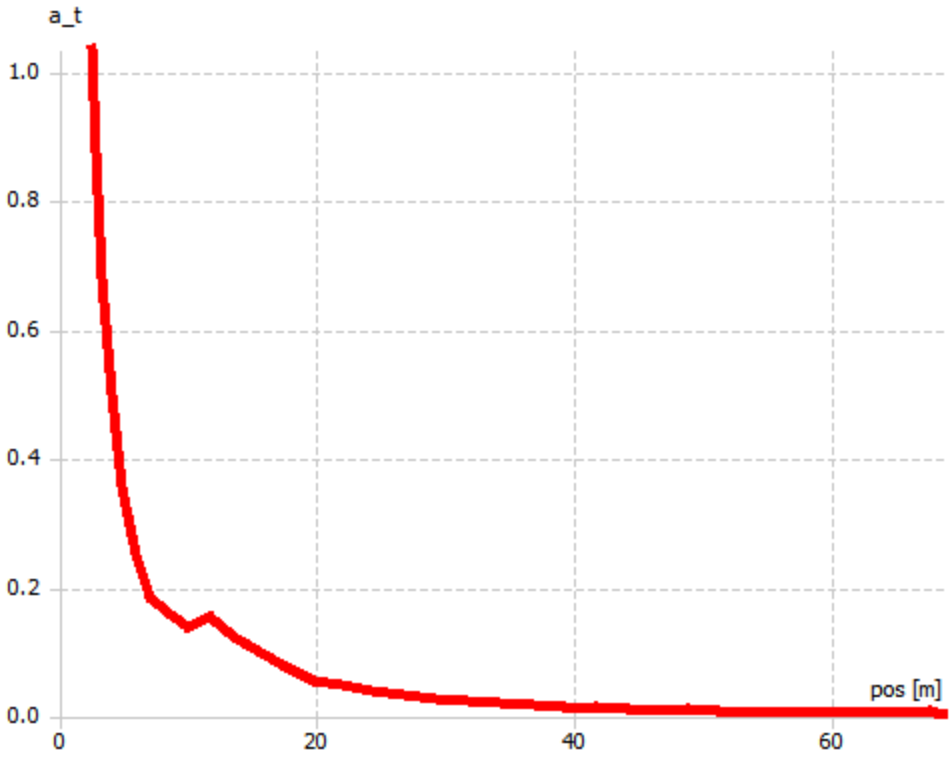

Figure 17:Tangential Induction Factor vs Span Graph

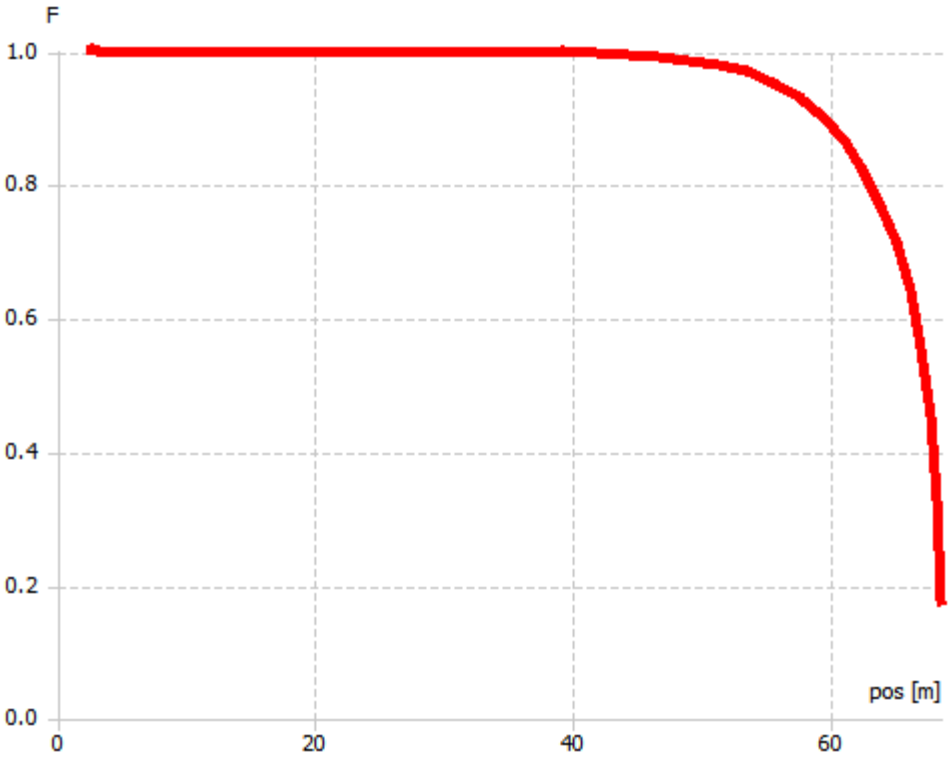

Figure 18:Prandtl Tip Loss Factor vs Span Graph

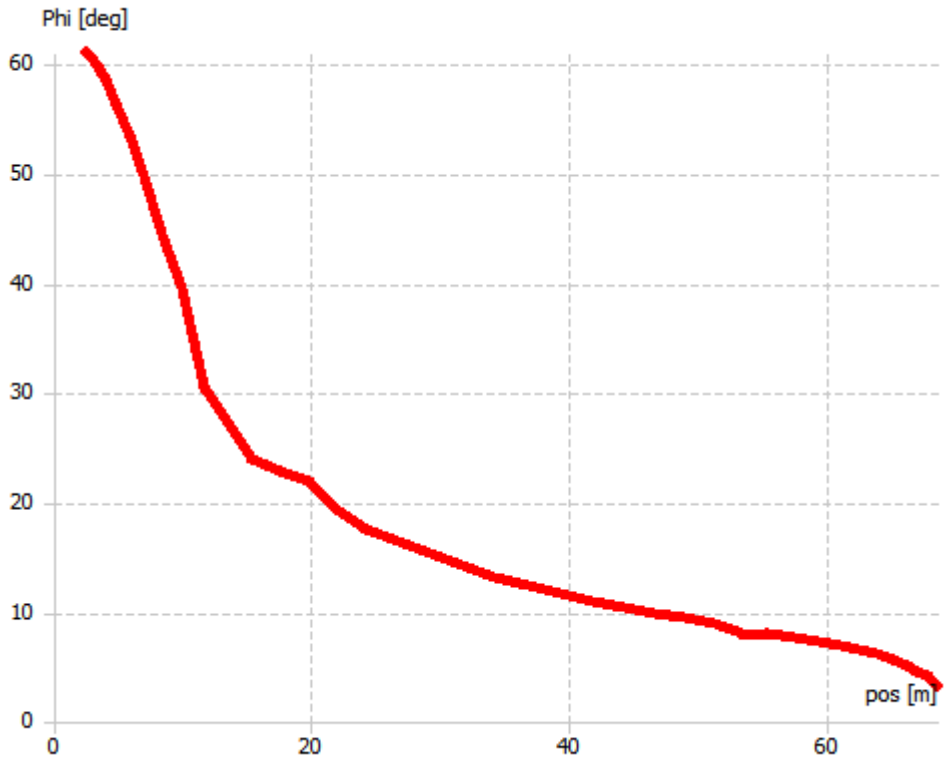

Figure 19: Inflow Angle vs Span Graph

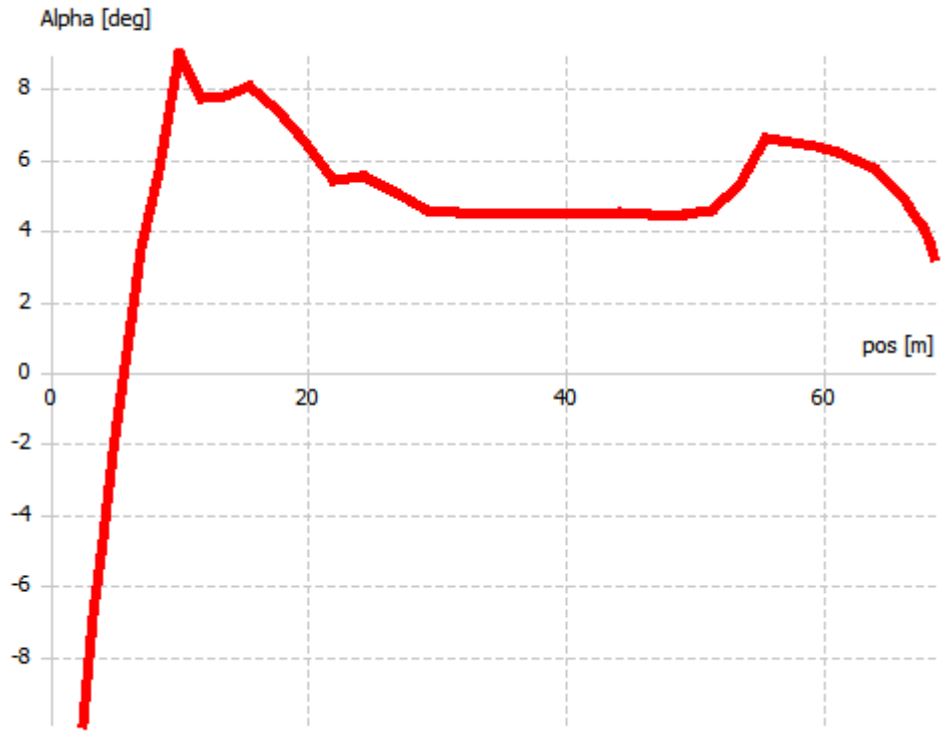

Figure 20: Angle of Attack vs Span Graph

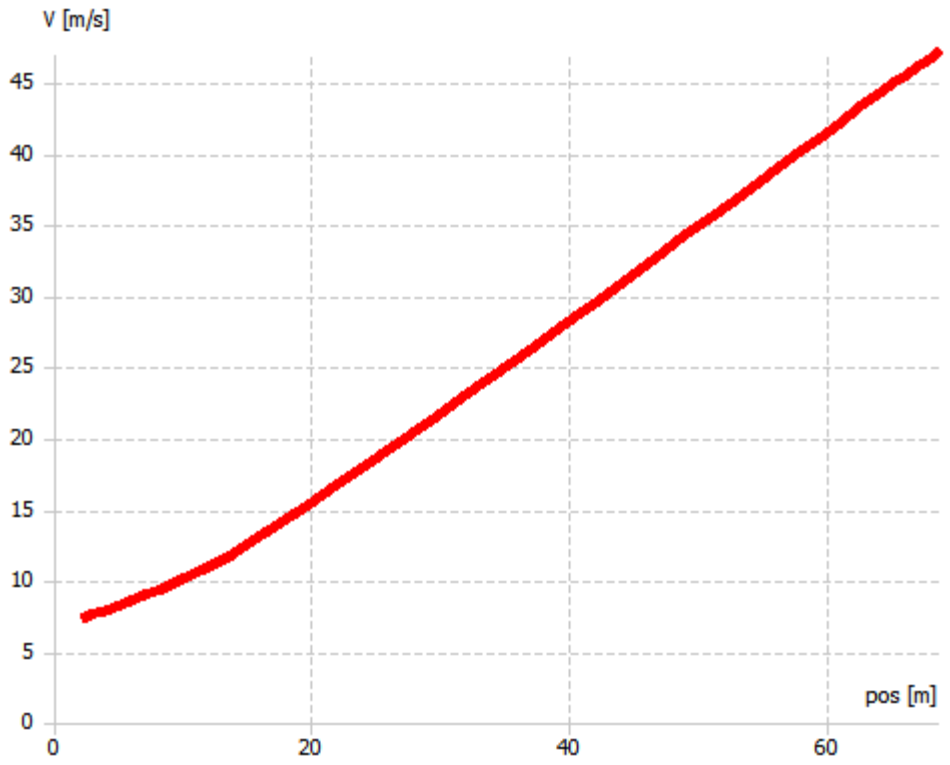

Figure 21: Resultant Velocity vs Span Graph

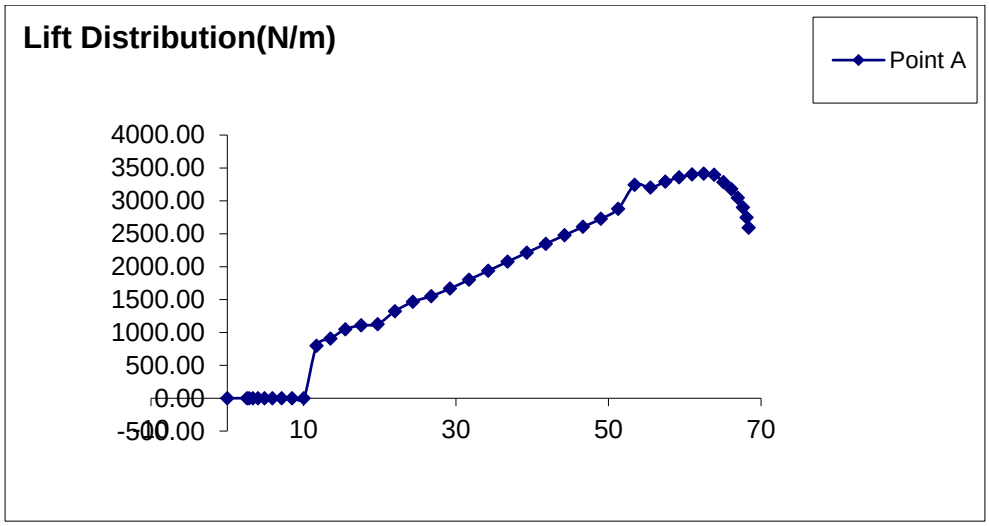

Figure 22:Lift Distribution for 66m Turbine Blade

PART 2
STRUCTURAL
DESIGN

2.1 MATERIALS SELECTION

The structural stresses could be extremely high for long wing turbine blades and in this study the blade length is 66m so it is very long and one should be careful to prevent the structural failures. Material selection is one of the main driving matters with structural geometry design. The materials for such large wind turbine blades are usually composites. Composites can be made from Glass fibers, carbon fibers, wood laminates, polyester resins and epoxies. Usually a composite is made by mixing a fiber which may also be called as reinforcement (which may be defined as an elongated stringy man-made material) with a polymer which also may be called as a matrix (which is a large molecule consisting of repeating units connected by covalent chemical bonds). Fibers can be carbonfiber, glassfiber and even wood. Glassfibers are heavier and weaker than carbonfibers but they are cheaper than carbonfibers. Usually in wind turbines for financial reasons glassfiber composites are used for shells and carbonfiber composites are used for spars. From [4] it is known that as glassfibers usually E-glass is used for wind turbines, although there is also another fiber which is stronger and which is called S-Glass, S-Glass is very expensive and not chosen in the market due to financial considerations. There comes a material called Hiper-tex which provides the strength of S-Glass for the price of E-Glass. This material is a new technology and we have found a Hiper-Tex Composite for Wind Turbines in the industry and used it for our wind turbine. This composite is HiPer-tex™ W 3030 UP Resin. The data of this composite material can be found in [5]. For our designs spar we have used carbonfiber and just used the general properties while testing the blades in Q-FEM. The values we have used in Q-FEM are given below:

Material	Density (kg/m^3)	Elastic Modulus (Pa)
Shell (HiPer-Tex Composite)	1950	4.8e+10
Spar (Carbonfiber Composite)	1600	1.35e+11

Table 4: The Material Properties

To be on the safe side we have thought that 1770 MPA Ultimate tensile strength is the limit for our structure. However actually Hiper-tex could withstand against up to 2250 MPA.

2.2 ANALYSIS

In Q-FEM by making optimization and arrangements for the weight and durability configuration below is obtained (Note that the positions of the stations in Table 6Table 4 and Table 5 can be seen from Table 3):

Station	Shell Thickness	Spar Thickness
1	0.05	0.08

2	0.05	0.08
3	0.02	0.08
4	0.018	0.08
5	0.016	0.08
6	0.014	0.07
7	0.012	0.06
8	0.01	0.05
9	0.008	0.04
10	0.006	0.03
11	0.004	0.02
12	0.002	0.01
13	0.001	0.01
14	0.001	0.01
15	0.001	0.01
16	0.001	0.01

Table 5: Structural Geometry

The geometry is given below:

WTMA-3000A66: WTMA-3000A66 Structural Model

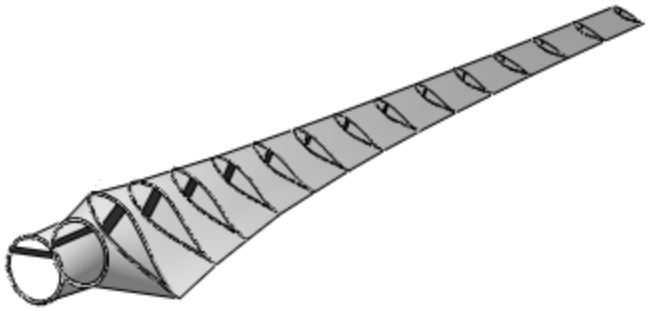

Flapwise Mode 1 Eigenfrequency: 5.59186 Hz Blade Mass: 211757 kg

Figure 23:Structural Design

For the maximum loading case for the speed of 25 m/s the data below is created:

Station	Normal Loading (N)	Tangential Loading (N)
1	3522.22	-1456.09
2	8361.21	-3701.81
3	9532.3	4168.14
4	8804.78	15702.4
5	8515.34	12883.9
6	9051.83	12178.2
7	8076.22	9815.08
8	6746.95	7139.33
9	5004.07	4648.74
10	2949.08	2411.64
11	1186.54	824.034
12	-480.147	-462.746
13	-1334.26	-998.836
14	-3419.54	-2266.68
15	-4895.14	-3046.86
16	-2654.02	-1617.04

Table 6: Loadings

The result graph from Q-FEM is given below:

WTMA-3000A66 Structural Model Loading Data

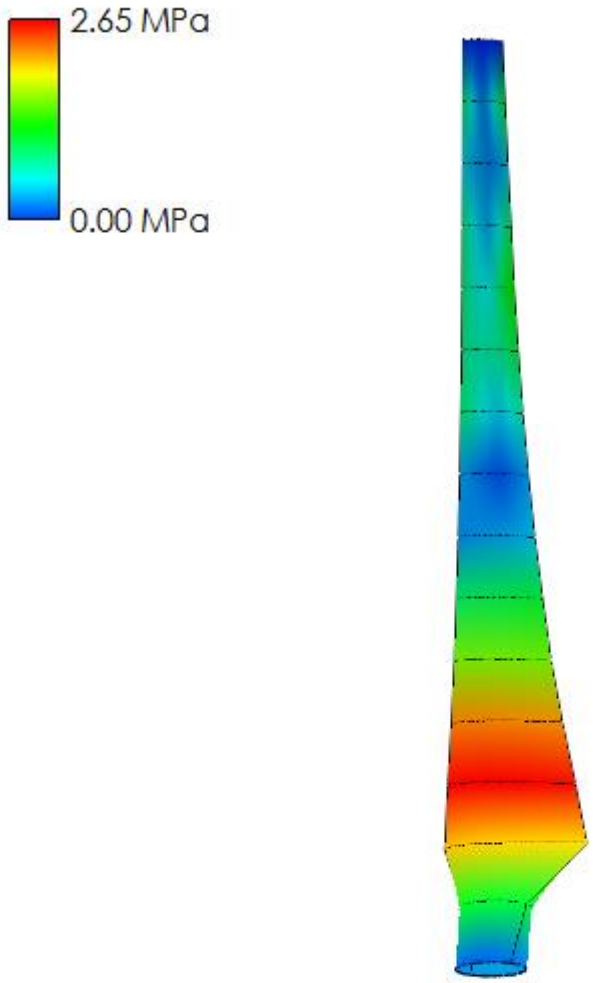

X Axis Tip Defl.-0.00203914 [m]

Z Axis Tip Defl. -0.00433922 [m]

Figure 24: Q-FEM Stress results for Blade

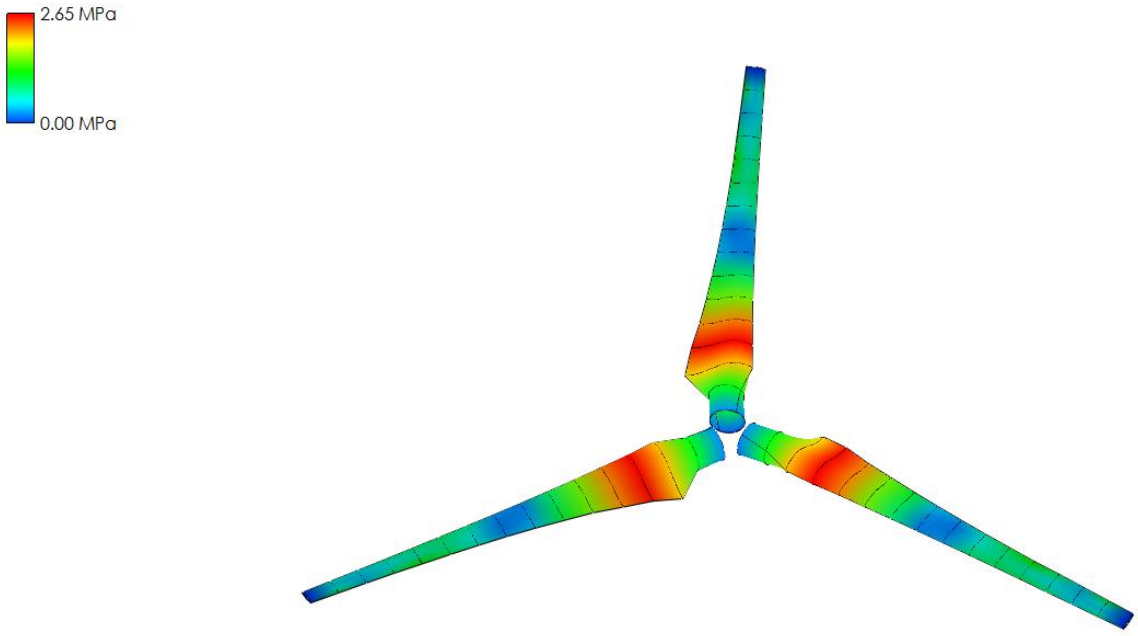

Figure 25: Q-FEM Stress results for the entire rotor

When the rotor is deflected it looks as below:

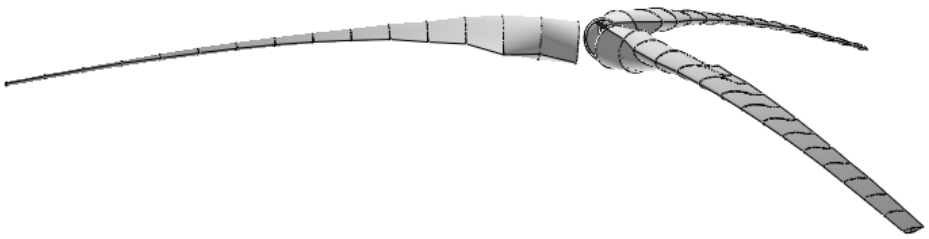

Figure 26: Deflected blades on the rotor

Then we decided to use ANSYS Structural for finite element analysis. Due to lack of time (as our team consists of 2 people) and lack of structural design knowledge (it is hard for us to determine the

thicknesses and positions of spars, shells etc.) we were able to analyze only the small model. As seen the maximum stress which occurs in Q-Blade does not exceed 1770 MPA. However while experimenting with Q-FEM we realized that it is not very accurate. In addition, Q-FEM did not give any results for mini model.

The forces are taken from Q-Blade for the mini model of our turbine then are applied to the blade model in ANSYS Structural:

x	Fn(N)	Ft(N)
0.0389	0.378303	0.14782
0.0778	0.113491	0.14782
0.1167	0.189151	0.14782
0.1556	0.264812	0.14782
0.1945	0.340472	0.14782
0.2334	0.416133	0.14782
0.2723	0.491793	0.14782
0.3112	0.567454	0.14782
0.3501	0.643114	0.14782
0.389	0.718775	0.14782
0.4279	0.794435	0.14782
0.4668	0.870096	0.14782
0.5057	0.945756	0.14782
0.5446	1.021417	0.14782
0.5835	1.097077	0.14782
0.6224	1.172738	0.14782
0.6613	1.248398	0.14782
0.7002	1.324059	0.14782

Table 7: These are the forces taken from the Q-Blade

Our Model in ANSYS Structural with BC's applied is given below:

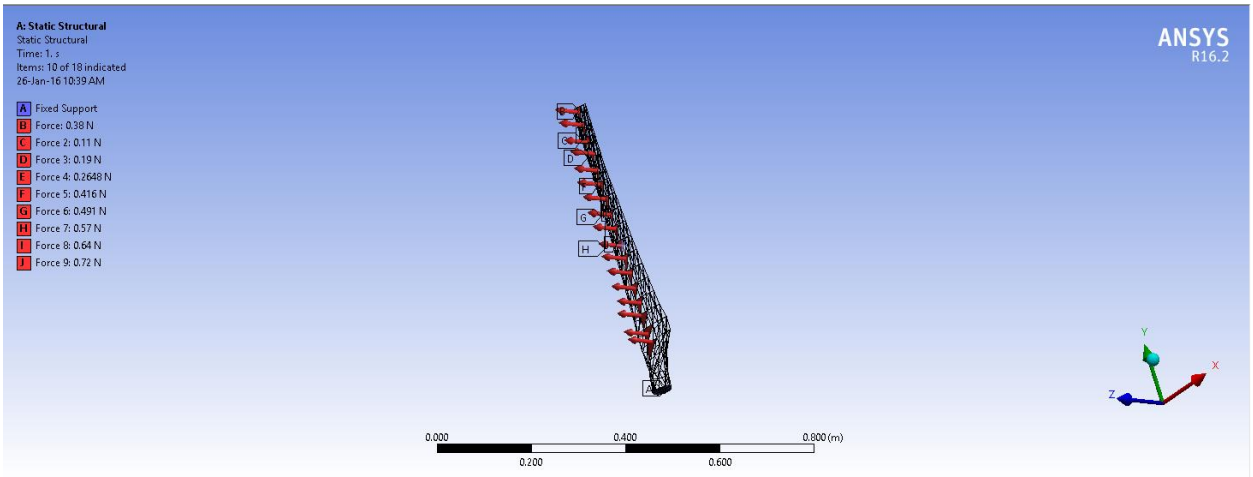

Figure 27:Structural Model with BC's

After doing the analysis the results are given below:

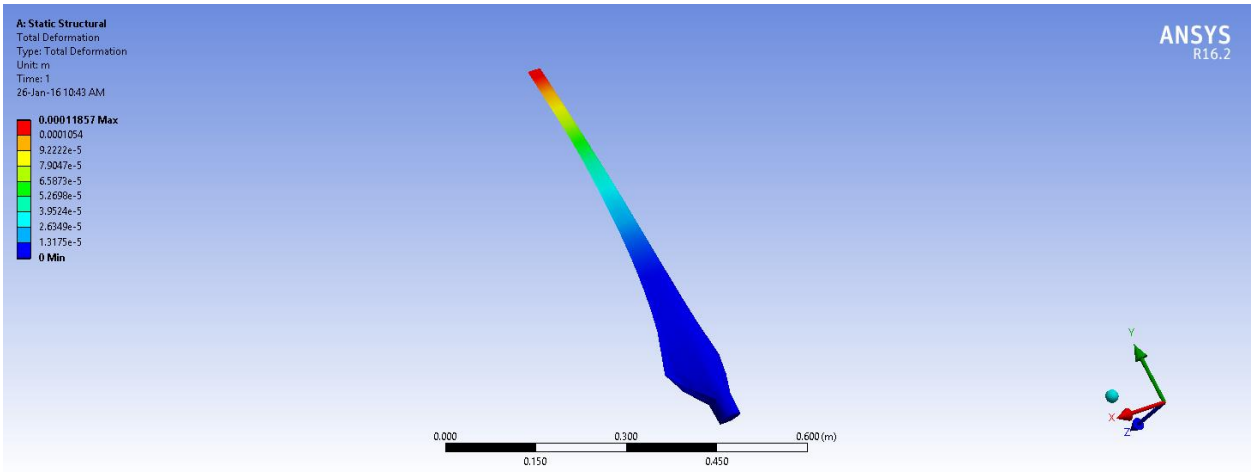

Figure 28: Total Deformation

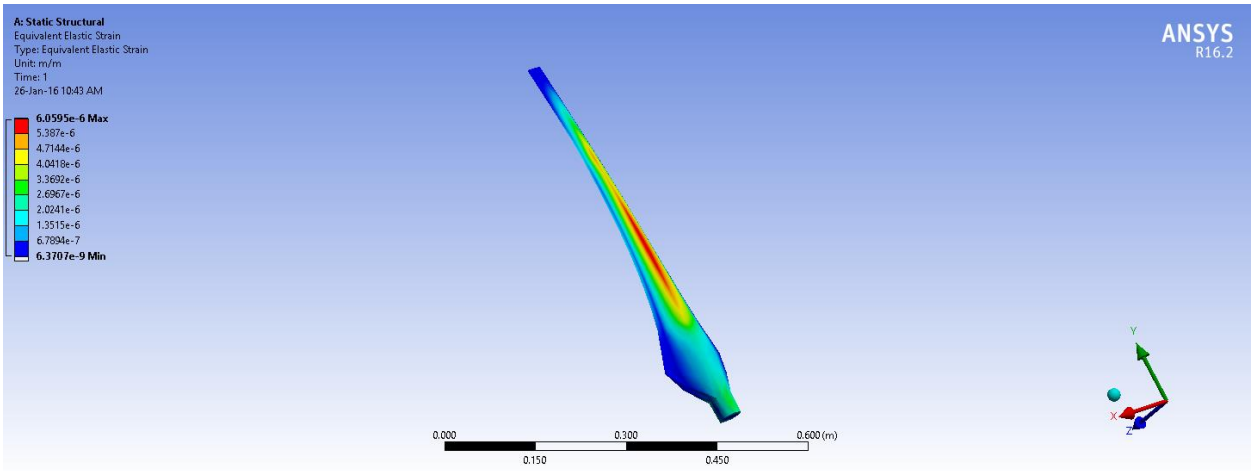

Figure 29: Equivalent Elastic Strain

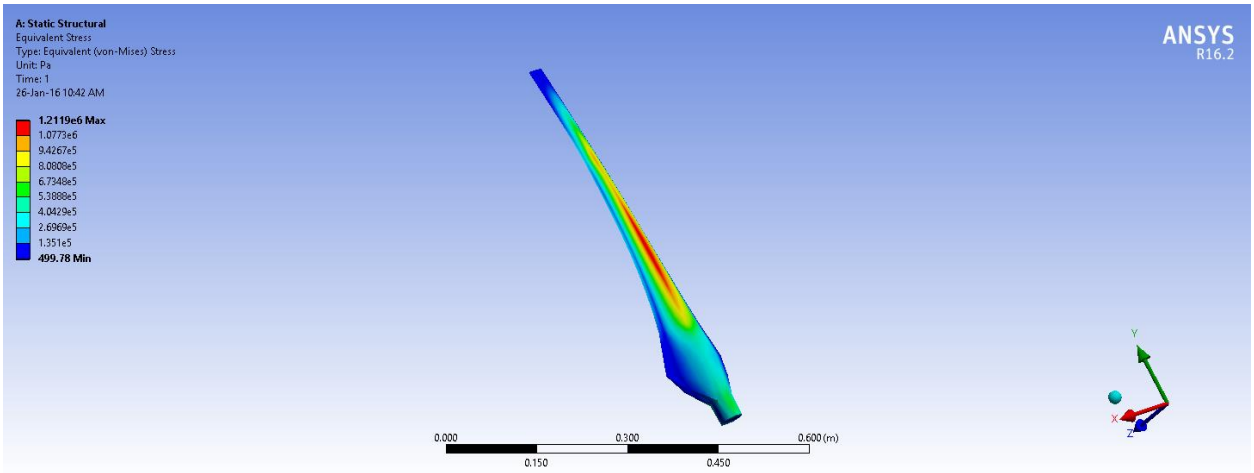

Figure 30: Equivalent (Von-Misses) Stress

Note that the max Von-Misses Stress is 1.2 MPa and ultimate tensile strength for Poyactic Acid is 50MPa, which means that our model could withstand against the winds.

3 SCALE MODEL

The chosen wind turbine will be produced as a scale model. Thus, our team has decided to study the scale model also. The scale model rotors diameter is 1.4m so our team has scaled down the turbine design and used the same procedure for the scale turbine model. The scale models rated power is chosen to be 300W although higher rated power can be achievable with the scale model 300W gave power curve which is closer to our original design.

Station	Pos (m)	Chord (m)	Twist (deg)	Airfoil
1	0	0.053	60.82	Circular
2	0.045	0.053	36.81	Circular
3	0.09	0.106	12.96	DU97W300LM
4	0.135	0.094	4.86	DU97W300LM
5	0.18	0.081	4.74	DU 91-W2-250
6	0.225	0.071	6.681	DU 91-W2-250
7	0.27	0.063	0.25	DU 93-W-210
8	0.315	0.056	-1.63	DU 93-W-210
9	0.36	0.05	-3.09	DU 93-W-210
10	0.405	0.046	-4.25	DU 93-W-210
11	0.45	0.042	-5.2	DU 93-W-210
12	0.495	0.038	-6	DU 93-W-210
13	0.54	0.036	-9.16	DU 95-W-180
14	0.585	0.034	-9.73	DU 95-W-180
15	0.629	0.031	-10.23	DU 95-W-180
16	0.674	0.03	-10.66	DU 95-W-180

Table 8: Twist and chord distribution of WTMA-3000A Scale Model

Scale model is assumed to be made from polylactic acid (One of the most common materials for 3D printer) to make it easier to produce. The properties required for polyactic acid.

Material	Density (kg/m^3)	Elastic Modulus (Pa)
Polyactic acid	1250	1e+10

Table 9:Properties of Polyactic Acid

Below are the figures given for the mini model performance parameters.

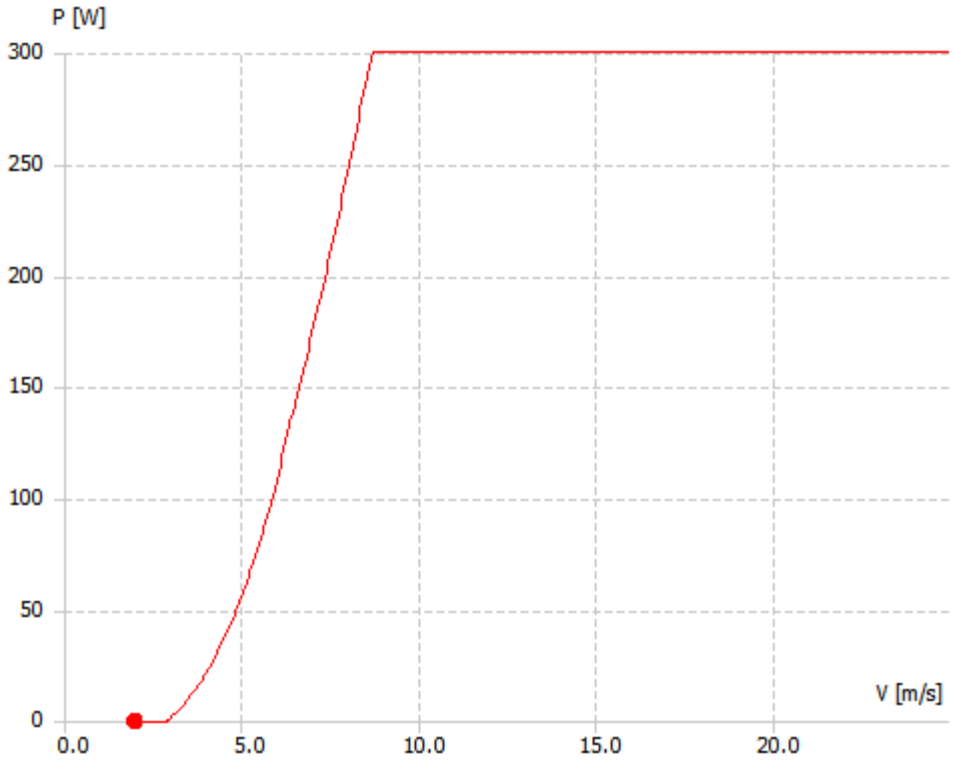

Figure 31: Power Curve of Small Scale Turbine Model

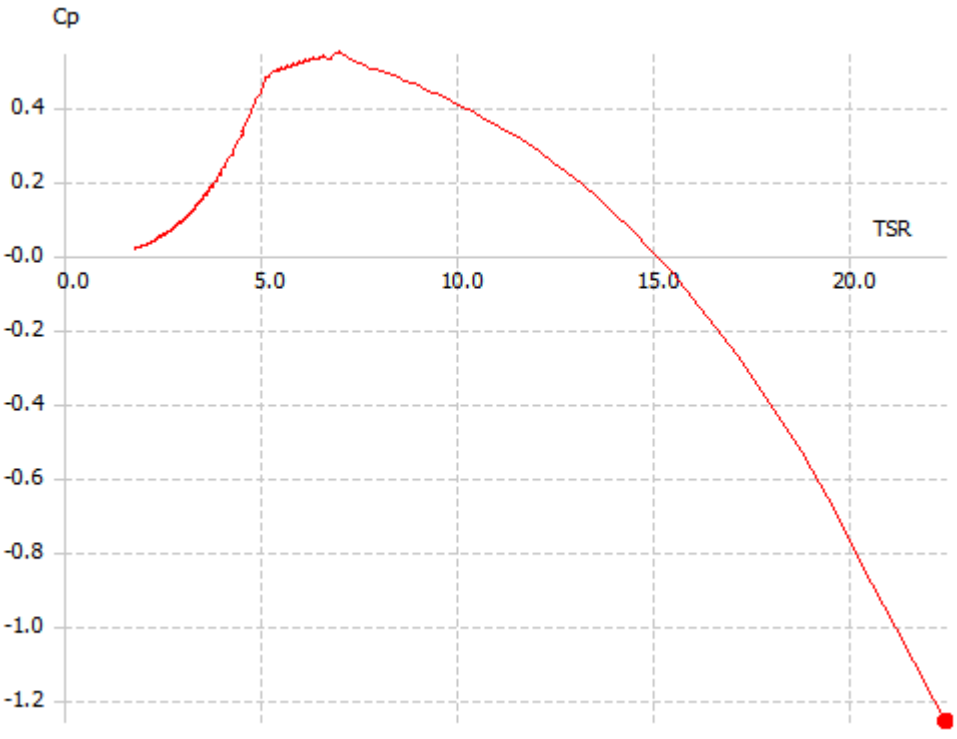

Figure 32: Power Coefficient vs Tip Speed Ratio of Scale Model

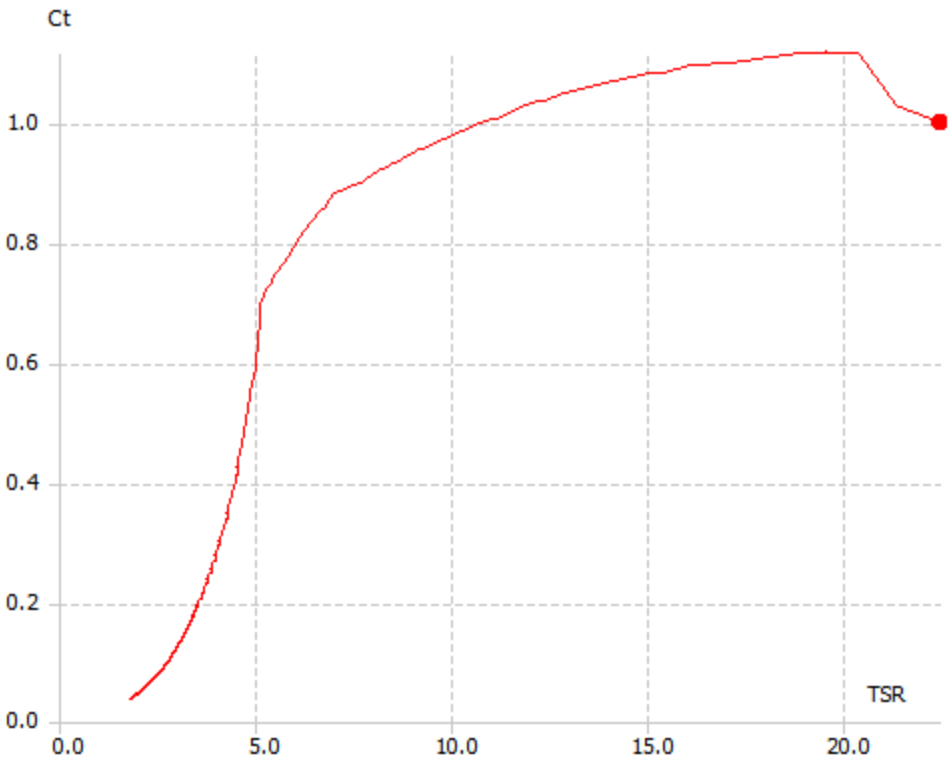

Figure 33: Thrust Coefficient vs Tip Speed Ratio Graph of Small Scale Turbine Model

The figures below are plotted for Freestream Velocity of 7.5 m/s.

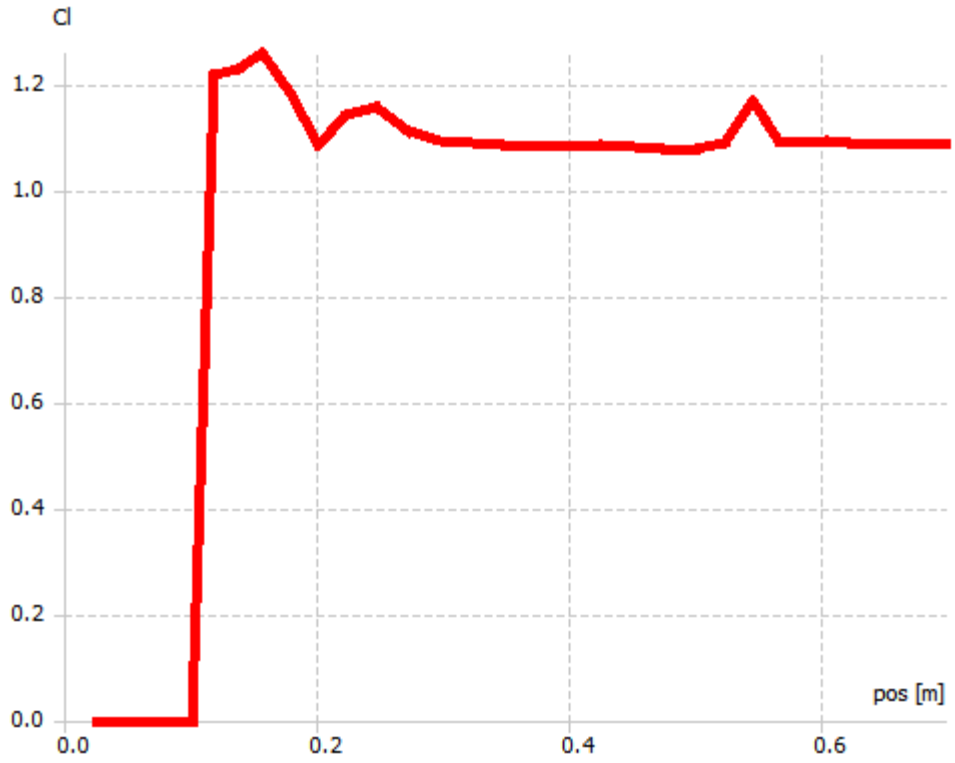

Figure 34: C_l vs Span Graph of Small Scale Model

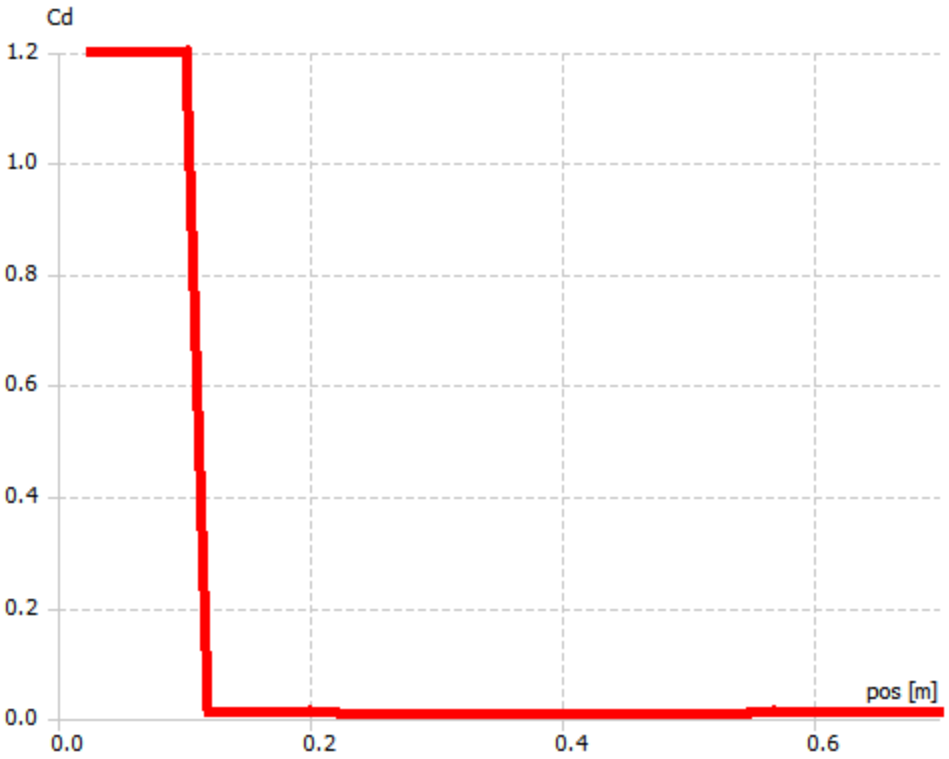

Figure 35: C_d vs Span Graph of Small Scale Model

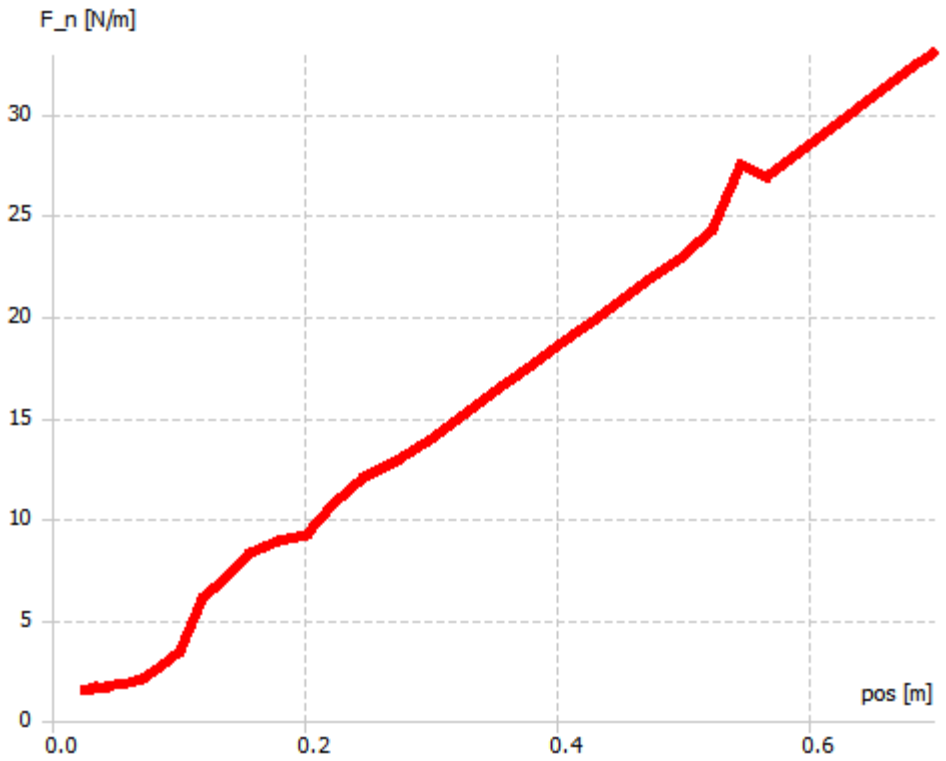

Figure 36: Axial Force vs Span Graph of Small Scale Model

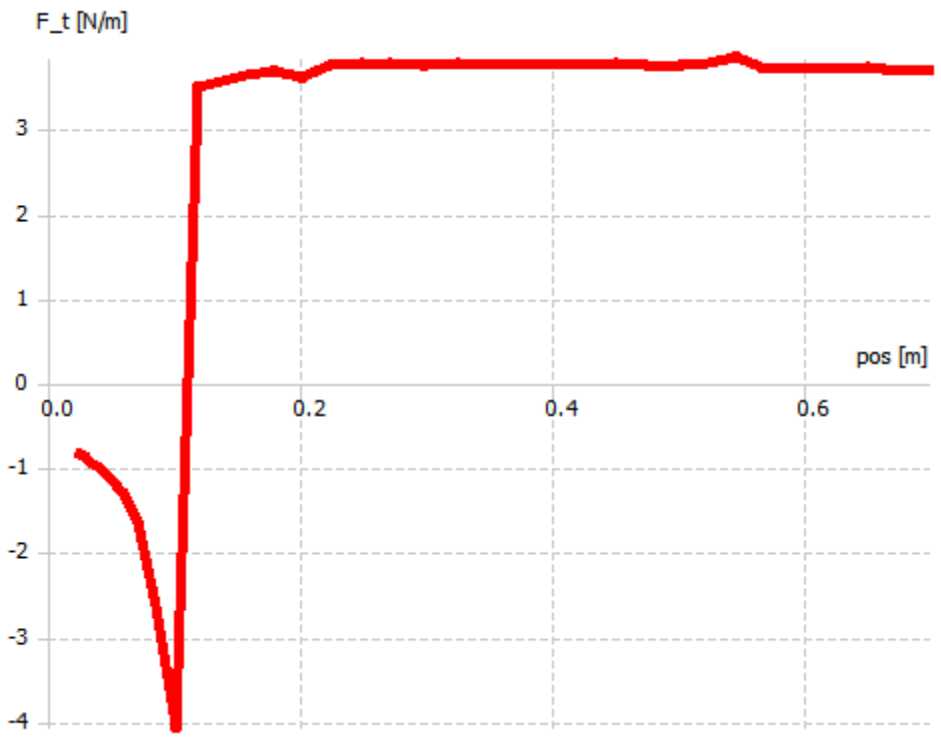

Figure 37: Tangential Force vs Span Graph of Small Scaled Model

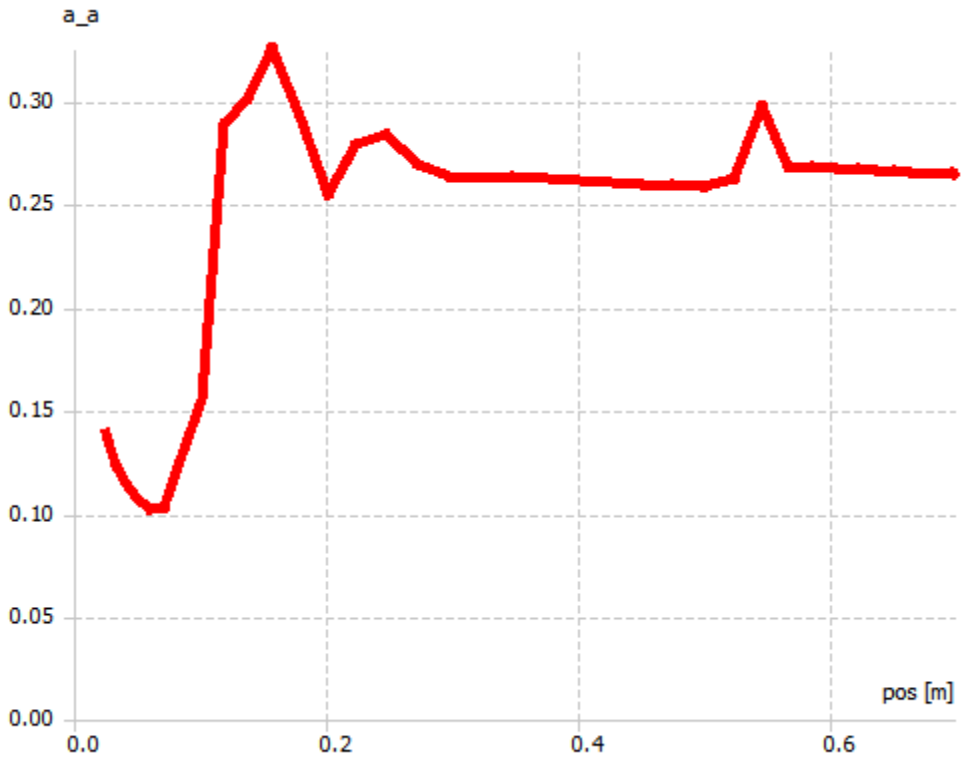

Figure 38: Axial Induction Factor vs Span Graph of Small Scale Model

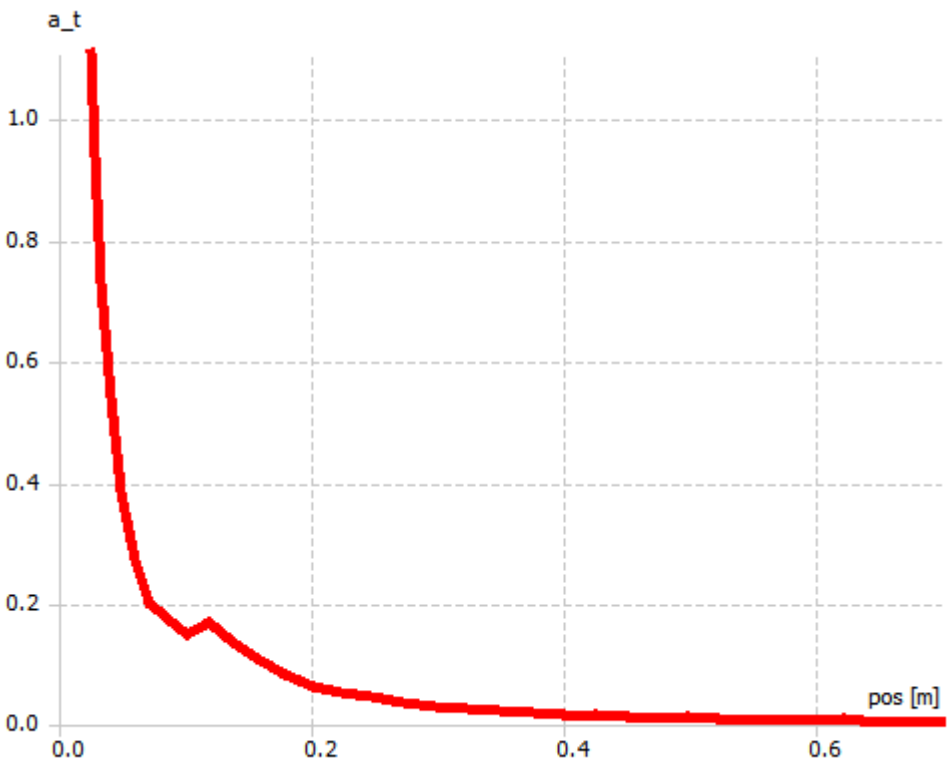

Figure 39: Tangential Induction Factor vs Span Graph of Small Scale Model

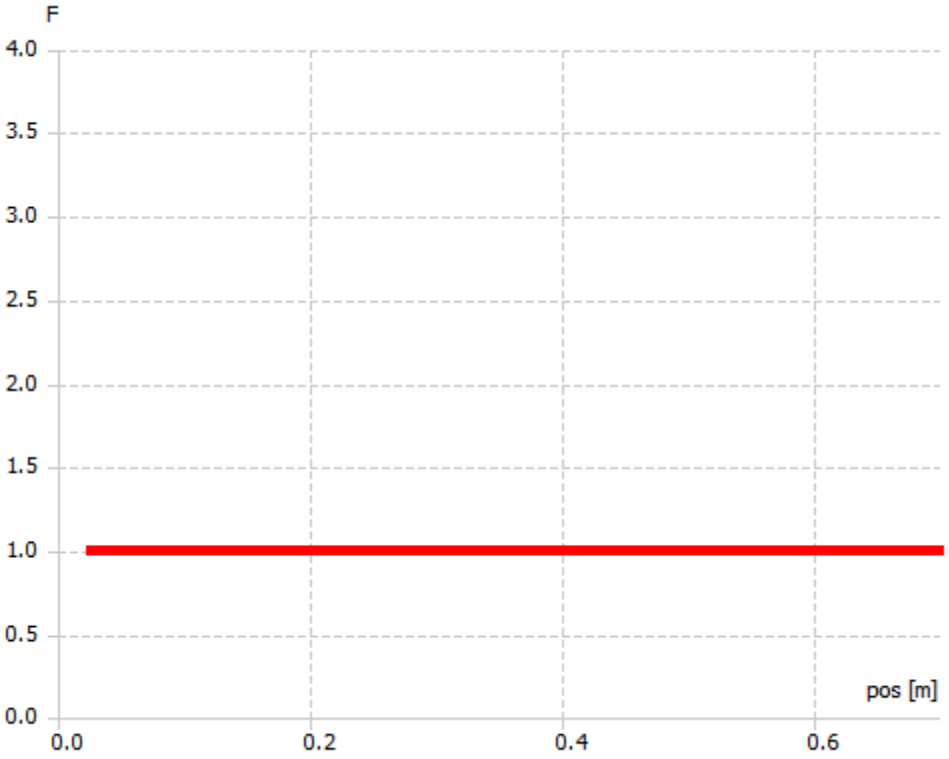

Figure 40: Prandtl Tip Loss Factor vs Span Graph of Small Scale Model

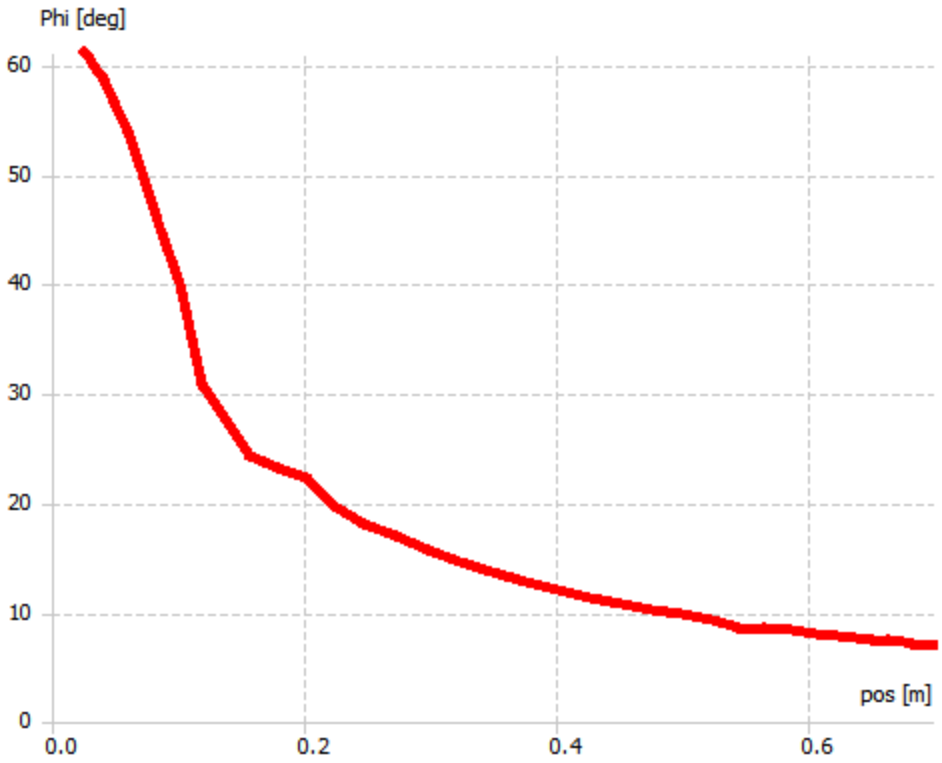

Figure 41: Inflow Angle vs Span Graph of Small Scale Model

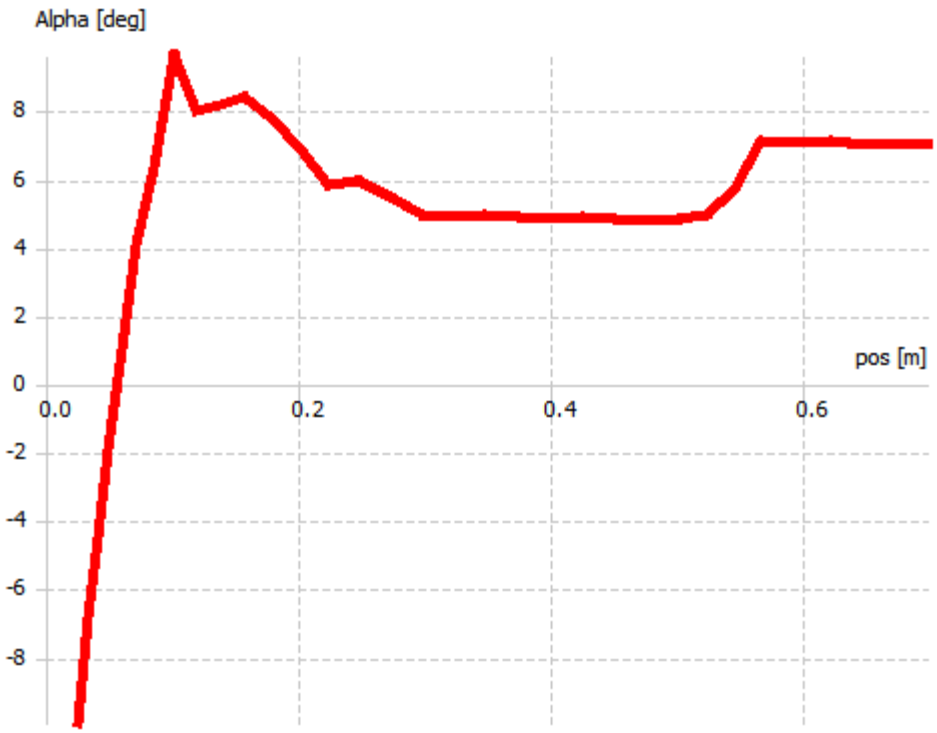

Figure 42: Angle of Attack vs Span Graph of Small Scale Model

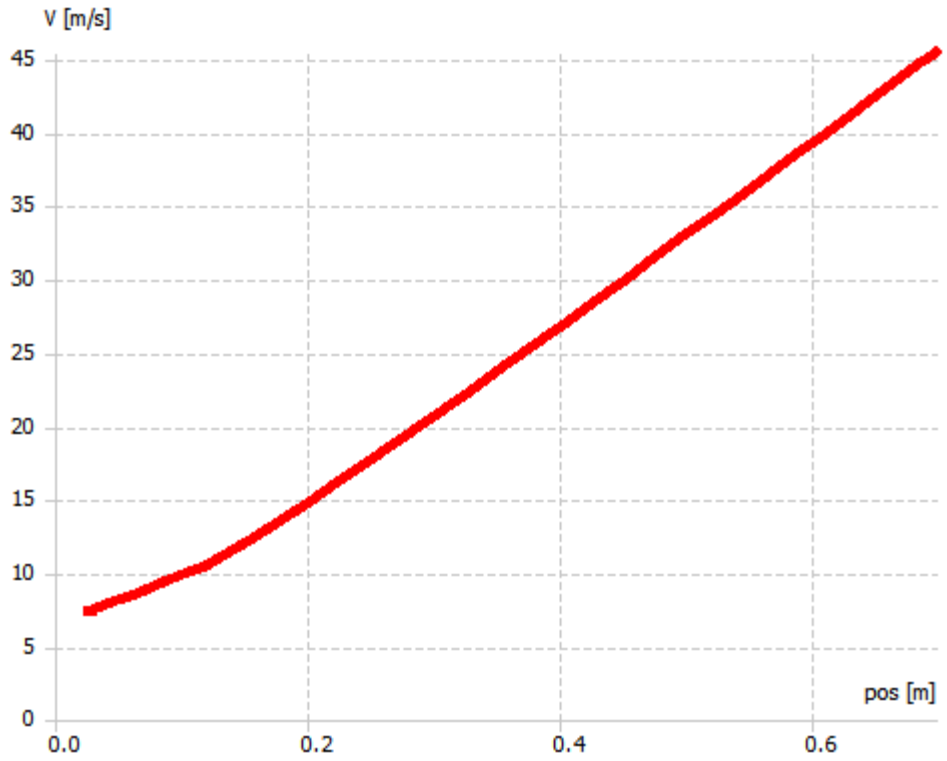

+

6

Figure 43: Resultant Speed vs Span Graph of Small Scale Model

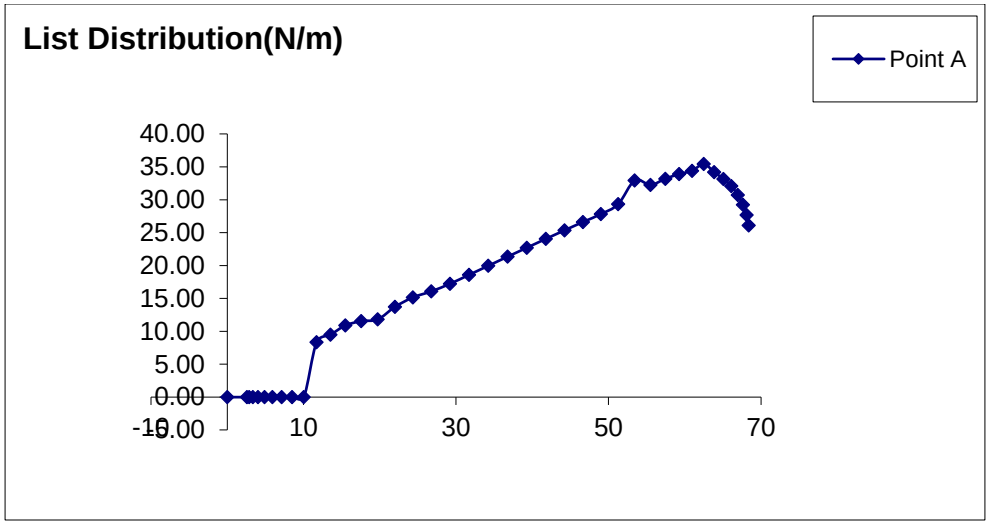

Figure 44: Lift Distribution for the Mini Model

4 CFD

CFD is done in the ANSYS Fluent. The rotor is created from blades taken from the Q-Blade. Unfortunately the CFD could not have done for the real model, but the scale model because of lack of time. The results of CFD are shown below:

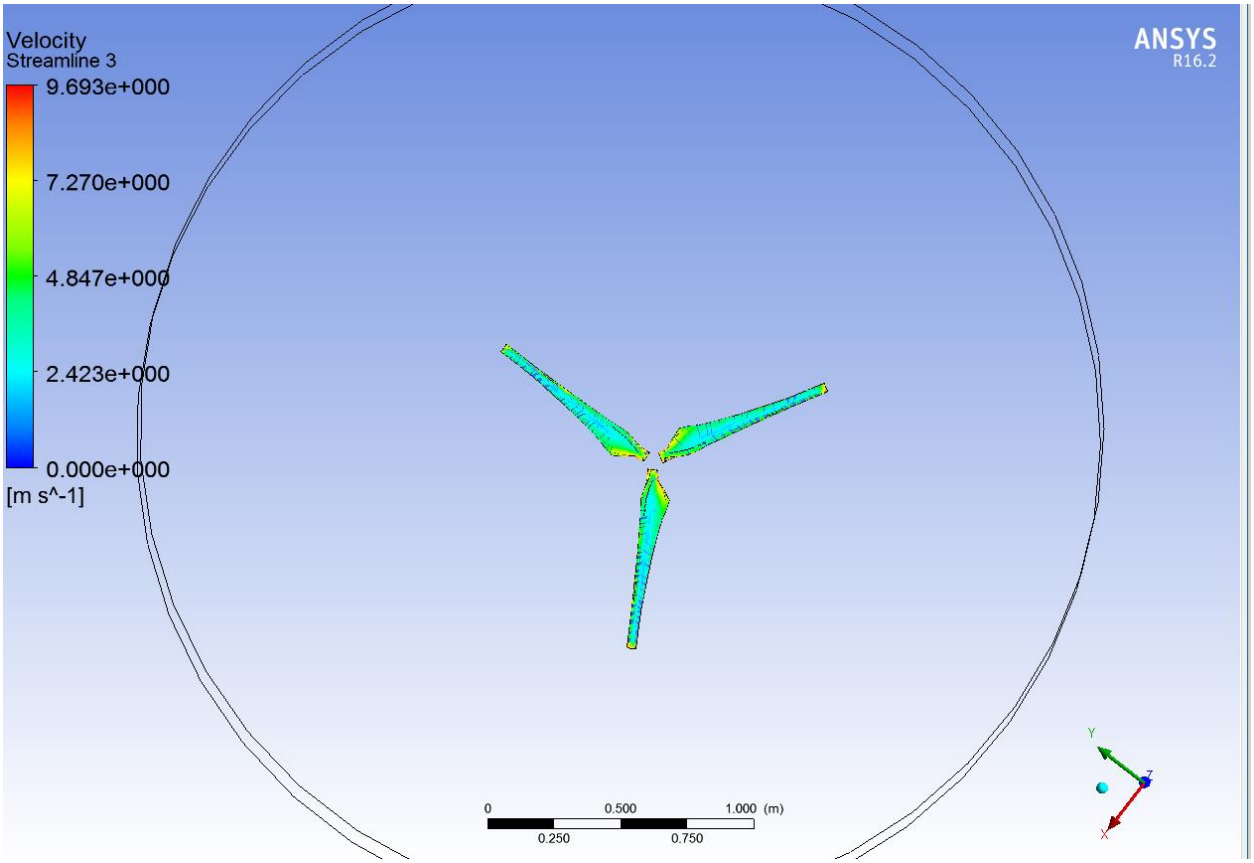

Figure 45:Velocity Streamlines for rotating blades

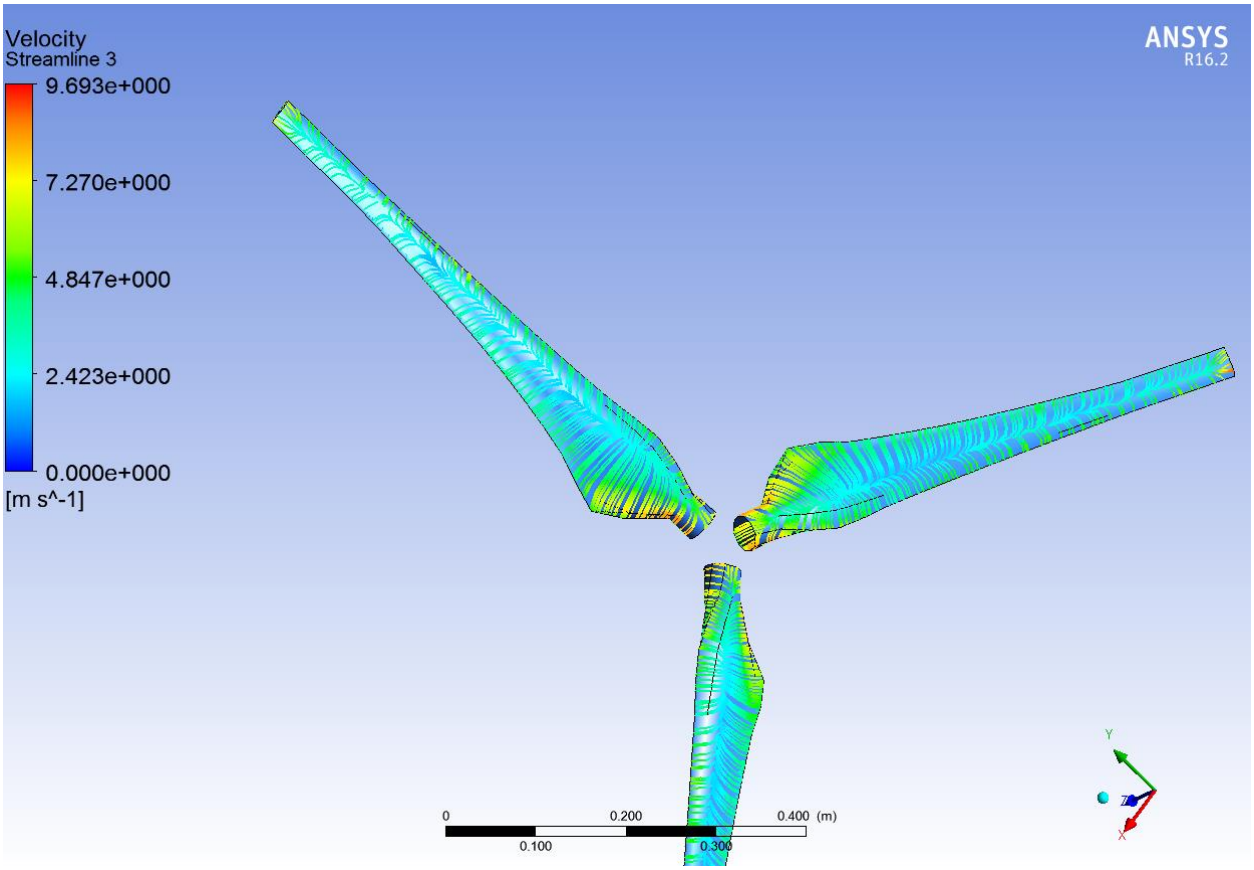

Figure 46: Velocity streamlines for rotating rotor, closer look

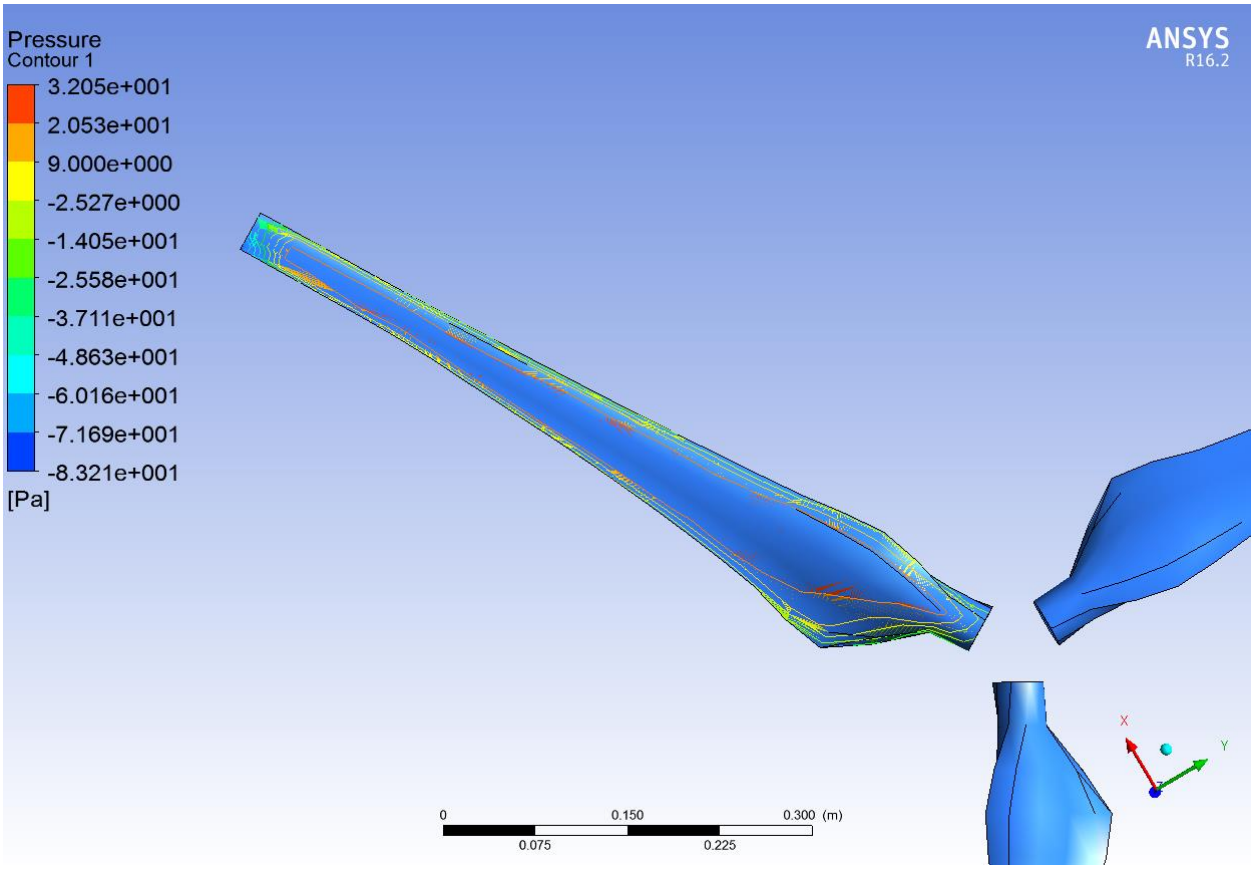

Figure 47: Close look-up for velocity contours

5 BIBLIOGRAPHY

[1] F. P. Incropera, D. P. DeWitt, T. L. Bergman, and A. S. Lavine, *Fundamentals of Heat and Mass Transfer*, vol. 6th. John Wiley & Sons, 2007.

[2] "What is the wind class of a wind turbine?," *Renewables First*, 2015. .

[3] W. a. Timmer and R. P. J. O. M. van Rooij, "Summary of the Delft University Wind Turbine Dedicated Airfoils," *J. Sol. Energy Eng.*, vol. 125, no. November 2003, p. 488, 2003.

[4] J. . F. MANWELL, J. G. MCGOWAN, and A. L. ROGERS, *WIND ENERGY EXPLAINED THEORY, DESIGN AND APPLICATION*, SECOND EDI. Wiltshire: WILEY, 2009.

[5] "HiPer-tex W 3030 Rovings." [Online]. Available: http://www.3b-fibreglass.com/wp-content/uploads/TDS-HiPer-tex-W-3030-for-Polyester-Vynilester-and-Epoxy-resin-2015-sans-trame-LR.pdf.